Circular Dichroism Studies of Molecular Recognition with Cyclophane Hosts in Aqueous Media

Jonathan E. Forman, Richard E. Barrans, Jr.,† and Dennis A. Dougherty*

Contribution No. 9092 from Arnold and Mabel Beckman Laboratories of Chemical Synthesis, Division of Chemistry and Chemical Engineering, California Institute of Technology, Pasadena, California 91125

Received May 18, 1995®

Abstract: Circular dichroism (CD) methods have been employed to study molecular recognition phenomena in water soluble cyclophane hosts such as **1** and **2**. The CD method is well suited to these systems and produces results that complement and expand upon previous NMR studies. The CD method operates at lower concentrations, allowing determinations of larger binding constants. Most importantly, when data concerning induced CD observed on binding achiral guests are analyzed using INDO/S coupled-oscillator calculations, valuable information concerning the binding conformations of the guest is obtained.

Introduction

Molecular recognition in aqueous media is of particular interest due its potential relevance to a variety of biological phenomena. A wide variety of synthetic receptors (hosts) have been shown to bind numerous substrates (guests) through various noncovalent interactions.[1−12] The primary method for studying binding interactions has been ^{1}H NMR.[13] NMR is a powerful tool, but it does have limitations, particularly when the hosts and guests have low solubilities and/or low critical aggregation concentrations (CACs). While UV spectroscopy can be used in some cases to overcome the solubility and CAC problems, UV spectra of cyclophane hosts are often relatively uninformative.

Work in our laboratories has focused on chiral cyclophane hosts, such as **1** and **2** (Figure 1).[12] These hosts bind cationic and neutral organic compounds through a variety of noncovalent interactions, including the cation-π interaction, hydrophobic binding forces, and weak electrostatic interactions. The intrinsic chirality of these hosts makes circular dichroism (CD) a potentially powerful probe of the binding interactions, thus

† Present address: Argonne National Laboratory; CHM/200, M019; Argonne, IL 60439.

® Abstract published in *Advance ACS Abstracts*, August 15, 1995.

(1) Diederich, F.; *Cyclophanes*; The Royal Society of Chemistry: Cambridge, UK, 1991.

(2) (a) Miyake, M.; Kirisawa, K.; Koga, K. *Chem. Pharm. Bull.* **1993**, *41*, 1211−1213. (b) Miyake, M.; Kirisawa, K.; Koga, K. *Heterocycles* **1993**, *36*, 1845−1849. (c) Miyake, M.; Kirisawa, K.; Koga, K. *Chem. Pharm. Bull.* **1992**, *40*, 3124−3126. (d) Miyake, M.; Kirisawa, K.; Koga, K. *Tetrahedron Lett.* **1991**, *32*, 7295−7298. (e) Lai, C. F.; Odashima, K.; Koga, K. *Chem. Pharm. Bull.* **1989**, *37*, 2351−2384. (f) Odashima, K.; Kawakami, H.; Miwa, A.; Sasaki, I.; Koga, K. *Chem. Pharm. Bull.* **1989**, *37*, 257−259. (g) Kawakami, H.; Yoshino, O.; Odashima, K.; Koga, K. *Chem. Pharm. Bull.* **1985**, *33*, 5610−5613. (h) Odashima, K.; Iitaka, Y.; Itai, A.; Koga, K. *Chem. Pharm. Bull.* **1985**, *33*, 4478−4484. (i) Odashima, K.; Spoga, T.; Koga, K. *Tetrahedron Lett.* **1981** *22*, 5311−5314. (j) Odashima, K.; Itai, A.; Iitaka, Y.; Koga, K. *J. Am. Chem. Soc.* **1980**, *102*, 2504−2505. (k) Soga, T.; Odashima, K.; Koga, K.; *Tetrahedron Lett.* **1980** *21*, 4351−4354.

(3) (a) Tabushi, L.; Yamamura, K.; Nonoguchi, H.; Hirotsu, K.; Higuchi, T. *J. Am. Chem. Soc.* **1984**, *106*, 2621−2625. (b) Tabushi, E.; Kimura, Y.; Yamamura, K. *J. Am. Chem. Soc.* **1981**, *103*, 6486−6492. (c) Tabushi, E.; Sasaki, H.; Kuroda, Y. *J. Am. Chem. Soc.* **1976**, *98*, 5727−5728.

(4) (a) Peterson, B. R.; Wallimann, P.; Carcanague, D. R.; Diederich, F. *Tetrahedron*, **1995**, *51*, 401−421. (b) Peterson, B. R.; Diederich, F. *Angew. Chem., Int. Ed. Engl.* **1994**, *33*, 1625−1628. (c) Smithrud, D. B.; Wyman, T. B.; Diederich, F. J. *J. Am. Chem. Soc.* **1991**, *113*, 5420−5426. (d) Smithrud, D. B.; Sanford, E. M.; Chao, I.; Ferguson, S. B.; Carcanague, D. R.; Evanseck, J. D.; Houk, K. N.; Diederich, F. *J. Pure Appl. Chem.* **1990**, *62*, 2227−2236. (e) Ferguson, S. B.; Seward, E. M.; Diederich, F.; Sanford, E. M.; Chou, A.; Inocenio-Szweda, P.; Knobler, C. B. *J. Org. Chem.* **1988**, *53*, 5593−5595.

(5) (a) Berscheid, R.; Lüer, I.; Seel, C.; Vögtle, F. In *Supramolecular Chemistry*; Balzzani, V., De Cola, L., Eds.; Kluwer Academic Publishers: The Netherlands, 1992; pp 71−76. (b) Seel, C.; Vögtle, F. *Angew. Chem., Int. Ed. Engl.* **1992**, *31*, 528−549. (c) Seel, C.; Vögtle, F. *Angew. Chem., Int. Ed. Engl.* **1991**, *30*, 442−444. (d) Ebmeyer, F.; Vögtle, F. In *Bioorganic Chemistry Frontiers*; Springer-Verlag: Berlin, 1990; Vol. 1, pp 145−158.

(6) (a) Bernardo, A. R.; Stoddart, J. F.; Kaifer, A. E. *J. Am. Chem. Soc.* **1992**, *114*, 10624−10631. (b) Goodnow, T. T.; Reddington, M. V.; Stoddart, J. F.; Kaifer, A. E. *J. Am. Chem. Soc.* **1991**, *113*, 4335−4337.

(7) (a) Meric, R.; Lehn, J.-M.; Visneron, J.-P. *J. Chem. Soc., Chem. Commun.* **1993**, 129−131. (b) Dhaenens, M.; Lehn, J.-M.; Visneron, J.-P. *J. Chem. Soc., Perkin Trans. 2* **1993**, 1379−1382. (c) Dhaenens, M.; Lehn, J.-M.; Fernandez, M.-J. *New J. Chem.* **1991**, *15*, 873−877. (d) Lehn, J.-M. *Angew. Chem., Int. Ed. Engl.* **1988**, *27*, 89−112. (e) Dhaenens, M.; Lacombe, L.; Lehn, J.-M.; Vigneron, J.-P. *J. Chem. Soc., Chem. Commun.* **1984**, 1097−1099.

(8) (a) Whitlock, B. J.; Whitlock, H. W. *J. Am. Chem. Soc.* **1994**, *116*, 2301−2311. (b) Cochran, J. E.; Parrott, T. J.; Whitlock, B. J.; Whitlock, H. W. *J. Am. Chem. Soc.* **1992**, *114*, 2269−2270. (c) Whitlock, B. J.; Whitlock, H. W. *J. Am. Chem. Soc.* **1990**, *112*, 3910−3915.

(9) (a) Schneider, H.-J.; Schiestel, T.; Zimmermann, P. *J. Am. Chem. Soc.* **1992**, *114*, 7698−7703. (b) Schneider, H.-J. *Angew. Chem., Int. Ed. Engl.* **1991**, *30*, 1417−1436. (c) Schneider, H.-J.; Güttes, D.; Scheider, U. *Angew. Chem., Int. Ed. Engl.* **1986**, *25*, 647−649.

(10) Webb, T. H.; Suh, H.; Wilcox, C. S. *J. Am. Chem. Soc.* **1991**, *113*, 8554−8555.

(11) (a) Araki, K.; Shimizu, H.; Shinkai, S. *Chem. Lett.* **1993**, 205−208. (b) Ikeda, A.; Shinkai, S. *Tetrahedron Lett.* **1992**, *33*, 7385−7388. (c) Murakami, Y.; Kikuchi, J.; Ohno, T.; Hirayama, T.; Hisaeda, Y.; Nishimura, H.; Snyder, J. P.; Steliou, K. *J. Am. Chem. Soc.* **1991**, *113*, 8229−8242. (d) Hisaeda, Y.; Ihara, T.; Ohno, T.; Murakami, Y. *Tetrahedron Lett.* **1990**, *31*, 1027−1030. (e) Murakami, Y.; Kikuchi, J.; Ohno, T.; Hirayama, T. *Chem. Lett.* **1989**, 881−884. (f) Shinmyozu, T.; Sakai, T.; Uno, E.; Inazu, T. *J. Org. Chem.* **1985**, *50*, 1959−1963.

(12) (a) Kearney, P. C.; Mizoue, L. S.; Kumpf, R. A.; Forman, J. E.; McCurdy, A.; Dougherty, D. A. *J. Am. Chem. Soc.* **1993**, *115*, 9907−9919. (b) McCurdy, A.; Jimenez, L.; Stauffer, D. A.; Dougherty, D. A. *J. Am. Chem. Soc.* **1992**, *114*, 10314−10321. (c) Stauffer, D. A.; Barrans, R. E., Jr.; Dougherty, D. A. *Angew. Chem., Int. Ed. Engl.* **1990**, *29*, 915−918. (d) Stauffer, D. A.; Barrans, R. E., Jr.; Dougherty, D. A. *J. Org. Chem.* **1990**, *55*, 2762−2767. (e) Stauffer, D. A.; Dougherty, D. A. *Science* **1990**, *250*, 1558−1560. (f) Petti, M. A.; Shepodd, T. J.; Barrans, R. E., Jr.; Dougherty, D. A. *J. Am. Chem. Soc.* **1988**, *110*, 6825−6840. (g) Shepodd, T. J.; Petti, M. A.; Dougherty, D. A. *J. Am. Chem. Soc.* **1988**, *110*, 1983−1985. (h) Stauffer, D. A.; Dougherty, D. A. *Tetrahedron Lett.* **1988**, *29*, 6039−6042. (i) Shepodd, T. J.; Petti, M. A.; Dougherty, D. A. *J. Am. Chem. Soc.* **1986**, *108*, 6085−6087.

(13) (a) Barrans, R. E., Jr.; Dougherty, D. A. *Supramolecular Chem.* **1994**, *4*, 121−130. (b) Wang, T. M.; Bradshaw, J. S.; Izatt, R. M. *J. Heterocyclic Chem.* **1994**, *31*, 1097−1114. (c) Wilcox, C. S. In *Frontiers in Suprmolecular Organic Chemistry and Photochemistry*; Schneider, H.-J., Dürr, H., Eds.; VCH: Weinheim, 1990. (d) Horman, I.; Dreux, B. *Anal. Chem.* **1983**, *55*, 1219−1221. (e) Creswell, C. J.; Allred, A. L. *J. Phys. Chem.* **1962**, *66*, 1469−1472.

0002-7863/95/1517-9213$09.00/0

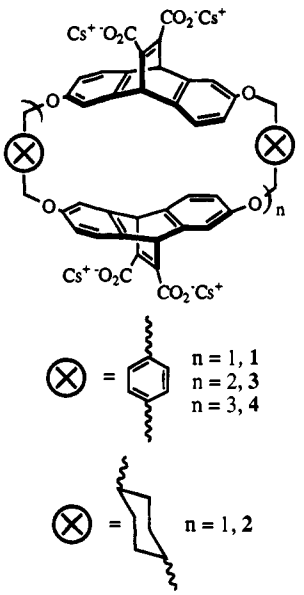

Figure 1. Hosts [(R,R) stereochemistry of ethenoanthracene units].

allowing the advantages of UV concentrations, but with more informative spectra. While CD has been used extensively for studying inclusion in cyclodextrins[14-18] and substrate binding in biological systems,[19] its use in studying chiral, synthetic hosts has been limited.[20-22]

In the present work we report the use of CD as an analytical tool for determining binding constants for our host-guest systems and show it to be a useful technique for studying guests that are problematic by NMR.[23] Along with **1** and **2**, "trimers" and "tetramers" (**3** and **4**, Figure 1)[12f] have been studied as well. These larger macrocyclic hosts have not been studied previously due to extremely low CACs. Binding constants for guests bound by these hosts are reported here for the first time. Most importantly, we show that for hosts **1** and **2**, analysis of induced CD seen in several achiral guests using coupled-oscillator calculations[24] can provide valuable insights into guest binding orientations. Where possible, guests appear to orient in the host cavity so as to maximize cation-π and hydrophobic interactions.

CD Spectra of Host 1 and Its Derivatives

The CD spectra of **1** and its higher oligomers (**3** and **4**) are all qualitatively similar to each other and to control molecule **5** (Figure 2, Table 1). Likewise, the spectra of host **2** and control molecule **6** are similar (Figure 3, Table 2). The chirooptical properties of these molecules appear to be dominated by the coupled oscillator mechanism (exciton optical activity),[24] but complete interpretation of the spectra is complicated by the large number of overlapping transitions between the component chromophores of the molecules. Semiempirical calculations (INDO/S) indicate that there are at least 17 $\pi \rightarrow \pi^*$ transitions

(14) Estimation of binding constants with CD: (a) Wulff, G.; Kubik, S. *Carbohydr. Res.* **1992**, *237*, 1-10. (b) Suzuki, M.; Kajtar, M.; Szejtli, J.; Vikmon, M.; Fenyvesi, E. *Carbohydr. Res.* **1992**, *223*, 71-80. (c) Schuette, J. M.; Ndou, T. T.; Warner, I. M. *J. Phys. Chem.* **1992** *96*, 5309-5314. (d) Suzuki, M.; Kajtar, M.; Szejtli, J.; Vikmon, M.; Fenyvesi, E.; Szente, L. *Carbohydr. Res.* **1991**, *214*, 25-33. (e) Patonay, G.; Warner, I. M. *J. Inclusion Phenom. Mol. Recognit. Chem.* **1991**, *11*, 313-322. (f) Barra, M.; Bohne, C.; Scaiano, J. C. *J. Am. Chem. Soc.* **1990**, *112*, 8075-8079. (g) Ishizuka, Y.; Nagawa, Y.; Nakanishi, H.; Akira, K. *J. Inclusion Phenom. Mol. Recognit. Chem.* **1990**, *9*, 219-225. (h) Breslow, R.; Greenspoon, N.; Guo, T.; Zarzycki, R. *J. Am. Chem. Soc.* **1989**, *111*, 8296-8297. (i) Hirai, H.; Toshima, N.; Hayashi, S.; Fujii, Y. *Chem. Lett.* **1983**, 643-646. (j) Yorozu, T.; Hoshino, M.; Imamura, M.; Shizuka, H. *J. Phys. Chem.* **1982**, *86*, 4422-4426.

(15) Determining guest orientations and conformations from analysis of CD curves: (a) Hamai, S.; Ikeda, T.; Nakamura, A.; Ikeda, H.; Ueno, A.; Toda, F. *J. Am. Chem. Soc.* **1992**, *114*, 6012-6016. (b) Buss, V.; Reichardt, C. *J. Chem. Soc., Chem. Commun.* **1992**, 1636-1638. (c) Kano, K; Yoshiyasu, K.; Yasouka, H.; Hata, S.; Hashimoto, S. *J. Chem. Soc., Perkin Trans. 2* **1992**, 1265-1259. (d) Buss, V. *Angew. Chem., Int. Ed. Engl.* **1991**, *30*, 869-870. (e) Kano, K.; Tatsumi, M.; Hashimoto, S. *J. Org. Chem.* **1991**, *56*, 6579-6585. (f) Kodaka, M. *J. Phys. Chem.* **1991**, *95*, 2110-2112. (g) Kobayashi, N.; Opallo, M. *J. Chem. Soc., Chem. Commun.* **1990**, 477-479. (h) Ata, M.; Kubozono, Y.; Suzuki, Y.; Aoyagi, M.; Gondo, Y. *Bull. Chem. Soc. Jpn.* **1989**, *62*, 3706-3708. (i) Ueno, A.; Moriwaki, F.; Osa, T.; Hamada, F.; Murai, K. *J. Am. Chem. Soc.* **1989**, *111*, 6391-6397. (j) Komiyama, M.; Takeshige, Y. *J. Org. Chem.* **1989**, *54*, 4936-4939. (k) Ueno, A.; Suzuki, I.; Osa, T. *J. Am. Chem. Soc.* **1988**, *110*, 4323-4328. (l) Kobayashi, N. *J. Chem. Soc., Chem. Commun.* **1988**, 918-919. (m) Kobayashi, N.; Zao, X.; Osa, T.; Kato, K.; Hanabusa, K.; Imoto, T.; Shirai, H. *J. Chem. Soc., Dalton Trans.* **1987**, 1801-1803. (n) Le Bas, G.; de Rango, C.; Rysanek, N.; Tsoucaris, G. *J. Inclusion Phenom. Mol. Recognit. Chem.* **1984**, *2*, 861-867. (o) Yamaguchi, H. *J. Inclusion Phenom. Mol. Recognit. Chem.* **1984**, *2*, 747-753. (p) Kobayashi, N.; Hino, Y.; Uneo, A.; Osa, T. *Bull. Chem. Soc. Jpn.* **1983**, *56*, 1849-1850. (q) Kobayashi, N.; Hino, H.; Hino, Y.; Uneo, A.; Osa, T. *J. Chem. Soc., Perkin Trans. 2* **1983**, 1031-1035. (r) Shimizu, H.; Kaito, A.; Hatano, M. *J. Am. Chem. Soc.* **1982**, *104*, 7059-7065. (s) Shimizu, H.; Kaito, A.; Hatano, M. *Bull Chem. Soc. Jpn.* **1981**, *54*, 513-519. (t) Shimizu, H.; Kaito, A.; Hatano, M. *Bull Chem. Soc. Jpn.* **1979**, *52*, 2678-2684. (u) Ikeda, N.; Yamaguchi, H. *Chem. Phys. Lett.* **1978**, *56*, 167-169. (v) Yamaguchi, H.; Ikeda, N.; Hirayama, F.; Uekama, K. *Chem. Phys. Lett.* **1978**, *55*, 75-76. (w) Harata, K.; Uedaira, H.; *Bull Chem. Soc. Jpn.* **1975**, *48*, 375-378. See also refs 14c and 14g.

(16) Determination of polarization directions of electronic transitions from analysis of induced CD curves: (a) Yamaguchi, M.; Higashi, M.; Oda, M. *Spectrochim. Acta* **1988**, *44A*, 547-548. (b) Kobayashi, N.; Minato, S.; Osa, T. *Makromol. Chem.* **1983**, *184*, 2123-2132. (c) Shimizu, H.; Kaito, A.; Hatano, M. *J. Am. Chem. Soc.* **1982**, *104*, 7059-7065.

(17) Extent of guest association with substituted cyclodextrins: (a) Kuwabara, T.; Nakamura, A.; Ueno, A.; Toda, F. *J. Phys. Chem.* **1994**, *98*, 6297-6303. (b) Yamaguchi, H.; Higashi, M. *J. Inclusion Phenom. Mol. Recognit. Chem.* **1987**, *5*, 725-728. (c) Kobayashi, N.; Osa, T. *Chem. Lett.* **1986**, 421-424. (d) Hira, H.; Toshima, N.; Uenoyama, S. *Bull. Chem. Soc. Jpn.* **1985**, *58*, 1156-1164.

(18) Solvent effects on the complex from CD data: Opallo, M.; Kobayashi, N.; Osa, T. *J. Inclusion Phenom. Mol. Recognit. Chem.* **1989**, *6*, 413-422.

(19) For example: (a) Huggins, J. P.; Ganzhom, A. J.; Saudek, V.; Pelton, J. T.; Atkinson, R. A. *Eur. J. Biochem.* **1994**, *221*, 581-593. (b) Gassner, G. T.; Ballou, D. P.; Landrum, G. A.; Whittaker, J. W. *Biochemistry* **1993**, *32*, 4820-4825. (c) Allen, B.; Blum, M.; Cunningham, A.; Tu, G. C.; Hofmann, T. *J. Biol. Chem.* **1990**, *265*, 5060-5065. (d) Reed, J.; Kinzel, V.; Kemp, B. E.; Cheng, H. C.; Walsh, D. A. *Biochemistry* **1985**, *24*, 2967-2973. (e) Kimura, T.; Bicknell-Brown, E.; Lim, B. T.; Nakamura, S.; Hasumi, H.; Koga, K.; Yoshizumi, H. *Dev. Biochem.* **1982**, *21*, 695-698. (f) Hofler, J. G.; Burns, R. O. *J. Biol. Chem.* **1978**, *253*, 1245-1251. (g) Orengo, A.; Patenia, D. M. Int. *J. Biochem.* **1976**, *7*, 423-432.

(20) Chiral calixarenes: (a) Arimura, T.; Shinkai, S. *Bull. Chem. Soc. Jpn.* **1991**, *64*, 1896-1900. (b) Arimura, T.; Kawabata, H.; Matsuda, T.; Muramatsu, T.; Satoh, H.; Fujio, K.; Manabe, O.; Shinkai, S. *J. Org. Chem.* **1991**, *56*, 301-306. (c) Arimura, T.; Kawabata, H.; Edamitsu, S.; Shinkai, S.; Manabe, O.; Muramatsu, T.; Tashiro, M. *Chem. Lett.* **1987**, 2269-2272. (d) Shinkai, S.; Arimura, T.; Satoh, H.; Manabe, O. *J. Chem. Soc., Chem. Commun.* **1987**, 1495-1496.

(21) Chiral cyclophane hosts: (a) Murakami, Y.; Hayashida, O.; Nagai, Y. *J. Am. Chem. Soc.* **1994**, *116*, 2611-2612. (b) Murakami, Y.; Hayashida, O.; Ono, K.; Hisaeda, Y. *Pure Appl. Chem.* **1993**, *65*, 2319-2324. (c) Murakami, Y.; Hayashida, O.; Ito, T.; Hisaeda, Y. *Pure Appl. Chem.* **1993**, *65*, 551-556. (d) Murakami, Y.; Ohno, T.; Hayashida, O.; Hisaeda, Y. *Chem. Lett.* **1991**, 1595-1598. (e) Murakami, Y.; Kikuchi, J.; Ohno, T.; Hayashida, O.; Kojima, M. *J. Am. Chem. Soc.* **1990**, *112*, 7672-7671.

(22) Chiral crown ethers: (a) Gu, D.; Kenney, B. D.; Brown, B. W. *Tetrahedron Lett.* **1994** *35*, 681-684. (b) Mack, M. P.; Hendrixson, R. P.; Palmer, R. A.; Ghirardelli, R. G. *J. Org. Chem.* **1983**, *48*, 2029-2035. (c) Malpass, G. D., Jr.; Palmer, R. A.; Ghirardelli, R. G. *Tetrahedron Lett.* **1980**, *21*, 1489-1492. (d) Kaneko, O.; Matsuura, N.; Kimura, K.; Shono, T. *Chem. Lett.* **1979**, 369-372. (e) Mack, M. P.; Hendrixson, R. P.; Palmer, R. A.; Ghirardelli, R. G. *J. Am. Chem. Soc.* **1976**, *98*, 7830-7832.

(23) Some general results of this work have been previously reported in ref 12a.

(24) (a) Tinoco, I., Jr. *Adv. Chem. Phys.* **1962**, *4*, 113-160. (b) Rosini, C.; Zandomeneghi, M.; Salvadori, P. *Tetrahedron Asymmetry* **1993**, *4*, 545-554. (c) Charney, E. *The Molecular Basis of Optical Activity-Optical Rotatory Dispersion and Circular Dichroism*; Robert E. Krieger Publishing Company: Malabar, FL, 1985. (d) Mason, S. F. *Molecular Optical Activity and the Chiral Discriminations*; Cambridge University Press: Cambridge, 1982.

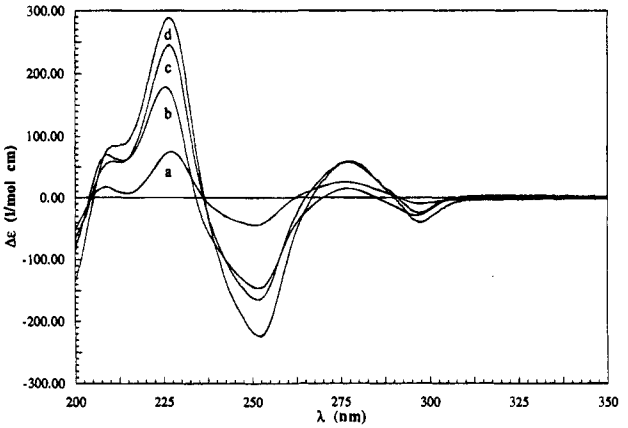

Figure 2. CD spectra of (a) $\mathbf{5_R}$, (b) $\mathbf{1_R}$, (c) $\mathbf{3_R}$, and (d) $\mathbf{4_R}$ in aqueous borate buffer (pH 9).

Table 1. Comparison of $\Delta\epsilon$ Data for Hosts **1**, **3**, and **4** and Control Molecule **5**[c]

$\mathbf{1_R}$		$\mathbf{3_R}$		$\mathbf{4_R}$		$\mathbf{5_R}$	
λ^a	$\Delta\epsilon^b$	λ^a	$\Delta\epsilon^b$	λ^a	$\Delta\epsilon^b$	λ^a	$\Delta\epsilon^b$
296	−35.0	296	−36.5	297	−39.1	297	−9.4
277	+15.7	277	+58.2	277	+60.0	276	+25.8
252	−151	251	−192	252	−224	251	−43.4
226	+168	227	+276	227	+289	227	+75.0
211 (sh)	+50.6	209	+77.1	211	+85	209	+17.9

[a] nm. [b] M^{-1} cm^{-1}. [c] Data are for (*R*,*R*)-stereochemistry of ethenoanthracene units.

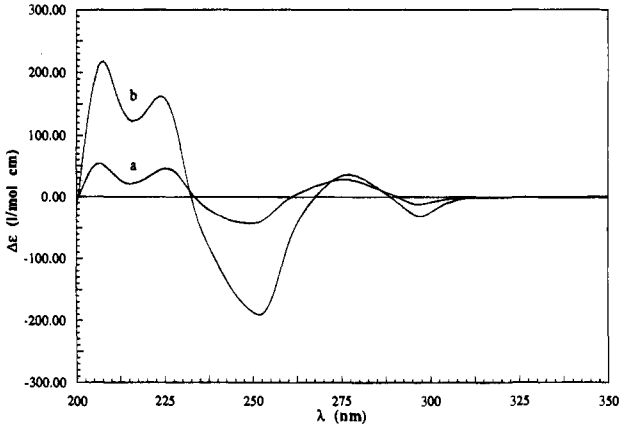

Figure 3. CD spectra of (a) $\mathbf{6_R}$ and (b) $\mathbf{2_R}$ in aqueous borate buffer (pH 9).

Table 2. Comparison of $\Delta\epsilon$ data for Host **2** and Control Molecule **6**[c]

$\mathbf{2_R}$		$\mathbf{6_R}$	
λ^a	$\Delta\epsilon^b$	λ^a	$\Delta\epsilon^b$
297	−30.9	297	−12.0
277	+36.6	276	+29.0
252	−190	250	−42.6
224	+163	225	+46.4
208	+218	206	+54.3

[a] nm. [b] M^{-1} cm^{-1}. [c] Data are for (*R*,*R*)-stereochemistry of ethenoanthracene units.

associated with the diacid of **6** in the 200−315 nm region of the CD spectrum. Calculations on α,α′-dimethoxy-*p*-xylene (**7**, a model for the linker chromophore) indicate two additional $\pi \rightarrow \pi^*$ transitions in the 200−250 nm region.

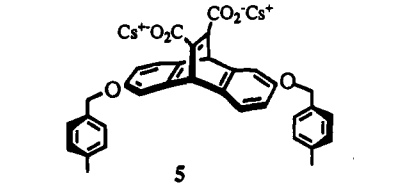

5

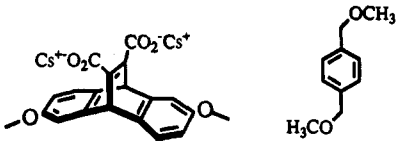

6

7

Structural Implications. This work has produced a verification of the previous assignment of the absolute stereochemistries of our host structures. In earlier work the absolute stereochemistries of the hosts had been assigned based on indirect and empirical observations.[12f] Circular dichroism spectra of exciton-coupled C_2-symmetric systems has been used extensively to assign absolute stereochemistry,[25] and our ethenoanthracene building block, **8**, is ideally suited for this type of analysis. Exciton-coupled CD has been discussed in detail by Harada and Nakanishi,[25] and our application of the method follows their analysis.

The "half-molecule", **8**, itself does not show a strong, easily assignable excitonic coupling in its CD spectrum despite the presence of the phenolic rings. Thus, two strongly interacting, but well isolated chromophores, needed to be placed onto the system. Following Nakanishi's protocol, we appended the *p*-(dimethylamino)benzoate chromophore (**9**, the arrow indicates direction of electronic transition dipole)[25] to our structures via the phenols to produce **10**.

As described in detail in the supporting information, molecular mechanics calculations[26-28] on **10** produced an unambiguous prediction concerning the relative orientation of the benzoate chromophores. This allowed the assignment of the absolute stereochemistry of **10**, and the assignment produced by CD agreed with that developed previously.[12f]

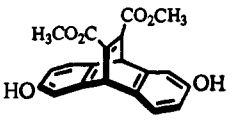

8

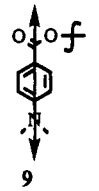

9

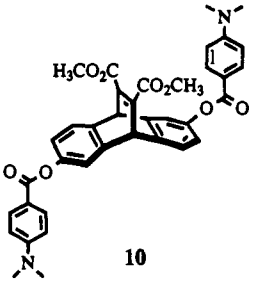

10

(25) Harada, N.; Nakanishi, K. *Circular Dichroic Spectroscopy-Exciton Coupling in Organic Stereochemistry*; University Science Books: Mill Valley, CA, 1983.

(26) BIOGRAF Version 2.2, Biodesign Inc., 1990.

(27) (a) Weiner, S. J.; Kollman, P. A.; Case, D. A.; Singh, U. C.; Ghio, C.; Algona, G.; Profeta Jr., S.; Weiner, P. *J. Am. Chem. Soc.* **1984**, *106*, 765−784. (b) Weiner, S. J.; Kollman, P. A.; Nguyen, D. T.; Case, D. A. *J. Comput. Chem.* **1986**, *7*, 230−252.

(28) Saunders, M.; Houk, K. M.; Wu, Y.-D.; Still, W. C.; Liptin, M.; Chang, G.; Guida, W. C. *J. Am. Chem. Soc.* **1990**, *112*, 1419−1427.

Measurement of Binding Constants with CD

Charts 1−3 show the guests studied and their respective binding constants measured with hosts **1**, **3**, and **4** using CD. The procedure for determining the equilibrium constant, K, from a set of CD spectra at different total host ($[H]_o$) and total guest ($[G]_o$) concentrations is not very different from the mathematics for obtaining K from NMR data, as in our previously described NMRfit and EMUL programs.[13a]

The Model: The basic assumption of our model is that the observed ellipticity at wavelength λ of a sample containing free host (H), free guest (G), and host−guest complex (HG) is

$$\theta_\lambda = gl(\Delta\epsilon_{H\lambda}[H] + \Delta\epsilon_{G\lambda}[G] + \Delta\epsilon_{HG\lambda}[HG]) \quad (1)$$

where θ_λ = the observed ellipticity at wavelength λ (generally measured in millidegrees, m°) $g = 2.30259 \times 45000/\pi$ m°M cm/deg, l = the cell path length, $\Delta\epsilon_{i\lambda}$ = the molar circular dichroism of species i at wavelength λ, and $[i]$ = the concentration of species i.

Substituting the expressions for total host concentration, $[H]_o = [H] + [HG]$, and total guest concentration, $[G]_o = [G] + [HG]$, into this equation results in

$$\theta_\lambda = gl\{\Delta\epsilon_{H\lambda}[H]_o + \Delta\epsilon_{G\lambda}[G]_o + E_\lambda[HG]\} \quad (2)$$

where

$$E_\lambda = \Delta\epsilon_{HG\lambda} - \Delta\epsilon_{H\lambda} - \Delta\epsilon_{G\lambda} \quad (3)$$

E_λ, an unknown quantity, is the change in molar ellipticity arising from complexation. The value of [HG] is determined by K, $[H]_o$, and $[G]_o$.

The task of the fitting procedure is to find K and E_λ to minimize

$$\chi^2 = \sum_c^S \sum_\lambda^L (\theta_{c\lambda\ \mathrm{calc}} - \theta_{c\lambda\ \mathrm{obs}})^2 \quad (4)$$

over the S experimental samples c and L observed wavelengths λ.

The best-fit value of E_λ corresponding to any K is immediately available by linear regression. The best-fit value of K, however, can only be found by iterating. We have developed a computer program (CDfit) that uses a Levenberg−Marquardt[29] procedure to accomplish this. Given the experimental data and an initial estimate of K, it returns the best-fit K and the set of best-fit E_λ. CDfit further converts the E_λ values into the best-fit CD spectrum of the pure host−guest complex.

Comparison with Other Methods

The method commonly used for obtaining association constants from CD spectra was developed by Rosen.[30] Rosen's method can be used for cases in which the host has an unknown number of noninteracting binding sites for the guest, but here we will only discuss its application to the case in which the host has exactly one site. Although this method was derived for cases in which the free guest has no CD over the wavelengths studied ($\Delta\epsilon_G = 0$), it is easily extended to cases for which $\Delta\epsilon_G \neq 0$.

This method requires measuring the CD of a set of samples in which $[H]_o$ is held constant and $[G]_o$ varies, or vice versa. Equation 2 rearranges to 5

Table 3. Comparison of Binding Constants for Host **1** Measured by CD and NMR

guest	$-\Delta G°$ [a] (CD)	$-\Delta G°$ [a,b] (NMR)
12	6.7	6.7
13	7.3	7.3
14	5.3	5.3
15	4.9	5.0

[a] kcal/mol. [b] These values are considered accurate to ±0.2 kcal/mol.

$$\frac{1}{[H]_{oc}}\left(\frac{\theta_{c\lambda}}{gl_c} - \Delta\epsilon_{H\lambda}[H]_{oc} - \Delta\epsilon_{G\lambda}[G]_{oc}\right) = E_\lambda\frac{[HG]_c}{[H]_{oc}} \quad (5)$$

in which the value on the right-hand side is E_λ multiplied by the fraction of host that is bound. For convenience, let us call this B, $B \equiv E_\lambda([HG]/[H]_o)$. A plot of B as a function of $[G]_o$ forms a rectangular hyperbola with an asymptote of E_λ. Near the origin of the plot, where $[G]_o$ approaches zero,[31] [HG] is equal to $[G]_o$, making the response of B to $[G]_o$ the same as its response to [HG]. Thus, a tangent line drawn to the initial region of the B vs $[G]_o$ plot is a graph of the definition of B, giving B as a function of [HG]. This definition readily inverts to yield [HG] as a function of B. Consequently, [HG], [H], and [G] are known from the measured value of B.

K is then estimated by Scatchard analysis.[32] A plot of $B/[G]$ vs B has a slope of $-K$ and a y-intercept of KE_λ, making these parameters readily available from the plot by linear regression. Weighting each point by $1/[G]_o$ corrects for transforming the experimental observations θ_{obs} to B.

For our systems, the CDfit analysis has several advantages over the Rosen/Scatchard analysis. CDfit does not require that $[H]_o$ be held constant; any combination of informative values of $[H]_o$ and $[G]_o$ may be used. No error is introduced by estimating the initial slope of the plot. The loss score χ^2 directly measures how well the experimental data are modeled, in contrast to the equation fitted in the Scatchard analysis. Furthermore, CDfit is better suited to analyze data recorded at a number of wavelengths. There is no need to estimate L initial slopes, nor does one need to reconcile L different estimates of K from L Scatchard plots. Only one estimate of K is returned, and it is the single value, in a least squares sense, most consistent with the experimental CD spectra in their entirety. Recording and fitting data at a number of wavelengths uses all of the available information in determining K. This not only makes the fitted K more reliable but also directly shows the effect of binding on the host and guest circular dichroism spectra.

The accuracy of our CD method is illustrated in the comparison of binding constants measured by this method and by our ^{1}H NMR method (Table 3). As shown in Table 3, the agreement with NMR lies within the 0.2 kcal/mol error bar range. In our hands the NMR method seems best suited in the range of 3.5 kcal/mol ≤ $-\Delta G°$ ≤ 8.0 kcal/mol. Likewise the CD method also has its limitations: 4.5 kcal/mol ≤ $-\Delta G°$ ≤ 10.5 kcal/mol; the lower limit of this range approaches 5.0−6.0 kcal/mol when the guest has strong UV absorbance in spectral regions that overlap with transitions in the host. Unlike our EMUL program,[13a] CDfit does not give a statistically meaningful estimate of error bars. Based on experimental observations and reproducibility of experiments, we estimate the error bars on a typical CD result (with good fit) to be ±0.2 kcal/mol (the same as in our NMR measurements).

(29) Press, W. H.; Flannery, D. P.; Teukolsky, S. A.; Vetterling, W. T. *Numerical Recipes: the Art of Scientific Computing*; Cambridge University: New York, 1986; pp 521−528.

(30) Rosen, A. *Biochem. Pharmacol.* **1970**, *19*, 2075−2081.

(31) The rigorous condition is $K([H]_o - [G]_o) \gg 1$.

(32) (a) Wyman, J.; Gill, S. J. *Binding and Linkage*; University Science Books: Mill Valley, CA, 1990; p 36. (b) Scatchard, G. *Ann. N. Y. Acad. Sci.* **1949**, *51*, 660−672.

Chart 1. Binding Constants ($-\Delta G°_a$, kcal/mol) for Guests Bound by Host **1** in Aqueous Borate Buffer (pH 9) Measured by CD

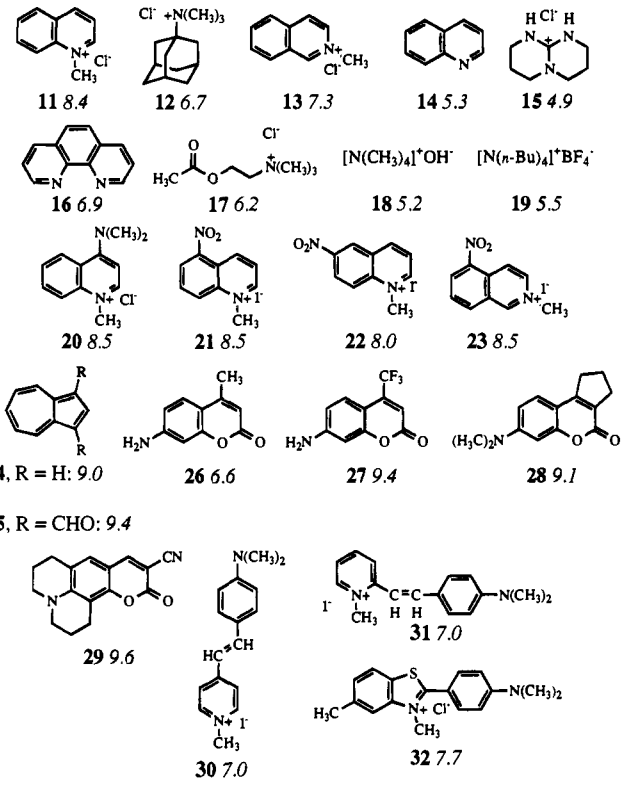

General Binding Results

The guests in Chart 1 nicely illustrate the range of binding constants that can be accurately determined using our CD method. As shown in Table 3, where comparisons are possible, agreement between binding constants determined by CD and by NMR is quite good. Guests **11**, **20**–**25**, and **27**–**29** deserve special mention as their binding constants lie above the upper limit of our NMR methods capability. Guests **24**–**29** are sparingly soluble in aqueous solution, with the concentrations of saturated solutions near or below the sensitivity limit of NMR. The high binding constants for these sparingly soluble guests can in part be attributed to strong hydrophobic forces. For azulenes, **24** and **25**, however, it is tempting to invoke a cation-π effect with the seven-membered ring of the guest being the cation (the binding orientation of these guests are described below).[12a,33]

One interesting comparison of guests is **26** vs **27**. These two coumarins differ only by the replacement of a methyl group (**26**) by a trifluoromethyl group (**27**), yet their binding constants with **1** differ by a remarkable 2.8 kcal/mol. We attribute this increase in binding to the inductive effect of the electron-withdrawing trifluoromethyl group. This leads to a stronger cation-π effect operating in the more electron-deficient **27**. There is probably also a difference in overall hydrophobicitics of **24** and **25**, but we expect this to be a relatively small effect. For example, log P values of toluene and α,α,α-trifluorotoluene differ by less than 0.1 units.[34]

The long wavelength charge transfer bands of **30**, **31**, and **32** exhibit bathochromic shifting in the presence of the host, and such behavior is consistent with the dye moving into a less polar environment (the host cavity).[35] Host **2** induces stronger red shifts than host **1**, consistent with the notion that the cavity of **2** is more hydrophobic. As with upfield shifting of guest protons in NMR studies, the spectral changes described here and the induced CD in the guests (see below) provide additional experimental confirmation of guest inclusion in our hosts. It should be noted that control studies with **5** and **6** showed induced CD in guests only under conditions in which either control molecule or guest was aggregated.

It was our intention to study only 1:1 host–guest complexation, but several studies suggested higher order complexes can also form with our hosts. With host **1**, dyes **33** and **34** show the expected induced CD ($\Delta\epsilon < 0$) and bathochromic shifting, but as host concentration increases relative to guest, the induced CD reverses sign. Preliminary data suggested multiple hosts binding to or aggregating about a single guest. Due to the complexity of the higher order system, studies of these guests were not further pursued. Control studies of the guests in Chart 1 in the presence of excess host **1** reveal no unusual behavior.

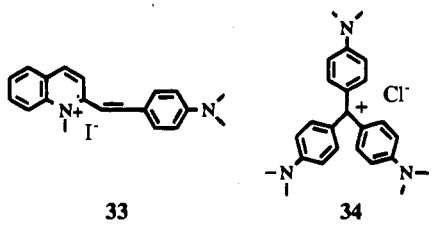

Host Binding Conformations

Figure 4 shows the best fit CD spectrum of complexes of host **1** with **11** and **12**—two prototypical guests for this system—in aqueous borate buffer compared to the CD spectrum of uncomplexed host. The spectra show significant *qualitative* differences. On the basis of modeling studies, we have previously argued that this host binds flat, naphthalene-like guests such as **11** in a C_2-symmetric, rhomboid conformation (Figure 5a) and large quaternary ammonium guests such as **12** in a D_2-symmetric toroid conformation (Figure 5b). The CD spectra provide the first experimental support for this model.[12f] The rhomboid shows a general decrease in magnitude of all Cotton effects (Figure 4a), while the toroid form is characterized by increasing intensity of lower wavelength Cotton effects (Figure 4b). This pattern holds up throughout the series of guests studied.

CD spectra of host **2** and its complexes with **11** and **12** show only subtle differences.[36] This suggests that it is the repositioning of the linkers (CD active in **1**, inactive in **2**) that is responsible for the observed CD changes accompanying host conformational changes. This assumption is consistent with calculated conformations of the hosts.[37]

In general, the guests shown in Chart 1 bind to host **1** in rhomboid-like conformations-toroid binding guests **12** and **19** are the only exceptions. This suggests that only very large, nearly spherical guests induce the toroid conformation. This is consistent with calculations[37] and a crystal structure[12a,38] which suggest a preference for the rhomboid conformation in host **1**.

(33) Dougherty, D. A.; Kearney, P. C.; Mizoue, L. S.; Kumpf, R. A.; Forman, J. E.; McCurdy, A. In *Computational Approaches in Supramolecular Chemistry*; Wipff, G., Ed.; NATO ASI Series, 1994.

(34) Leo, A.; Hansch, C.; Elkins, D. *Chem. Rev.* **1971**, *71*, 525–616.

(35) (a) Silverstein, R. M.; Bassler, G. C.; Morrill, T. C. *Spectrometric Identification of Organic Compounds*; John Wiley and Sons: New York, 1974. (b) Reichardt, C. *Chem. Rev.* **1994**, *94*, 2319–2358.

(36) The $\Delta\epsilon$ values for the host **2** complexes come from single spectra of solutions containing known amounts of host and guest; using previously measured binding constants ($-\Delta G°_a$ = 6.3 kcal/mol for guest **11** and 5.5 kcal/mol for guest **12**)[12f] and measured $\Delta\epsilon$ values for free host, the host–guest complex spectra were calculated from the measured spectra.

(37) Kumpf, R. A.; Dougherty, D. A. Unpublished results.

(38) Forman, J. E.; Marsh, R. E.; Schaefer, W. P.; Dougherty, D. A. *Acta. Crystallogr. Section B* **1993**, *B49*, 892–896.

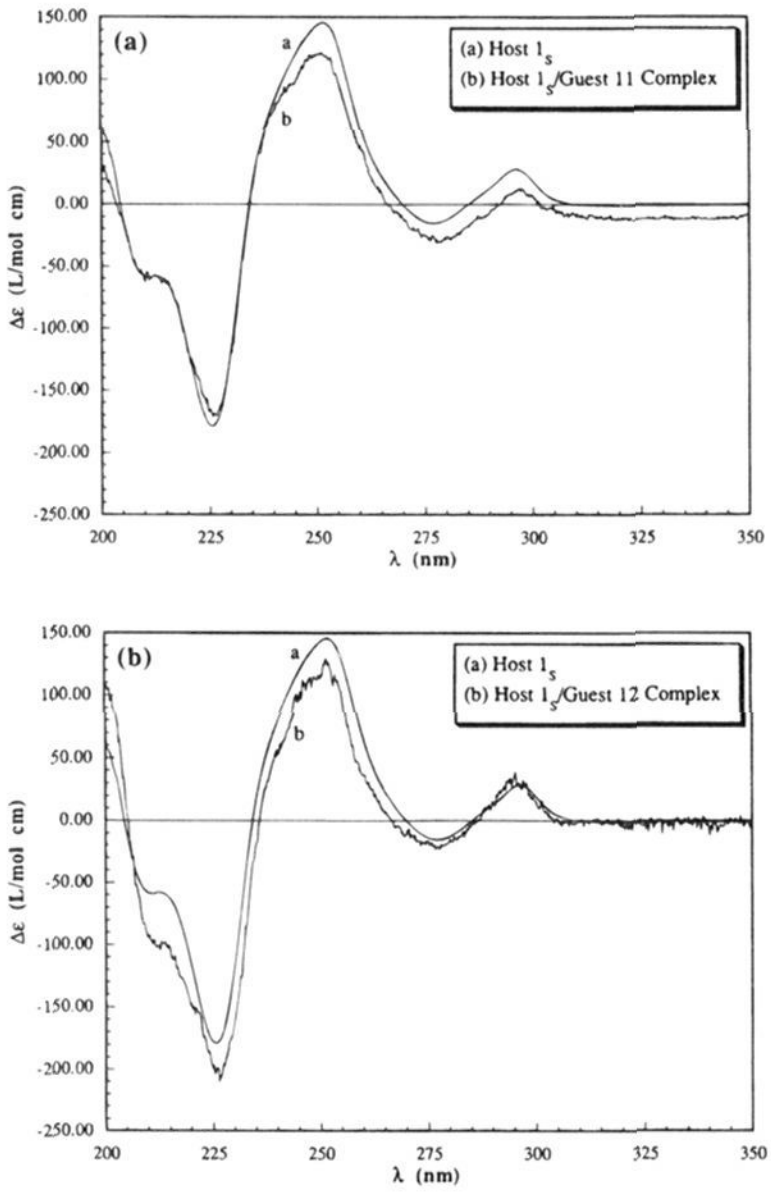

Figure 4. Best fit CD spectra of host $\mathbf{1_S}$ and its complexes with (a) guest **11** and (b) guest **12** in aqueous borate buffer (pH 9).

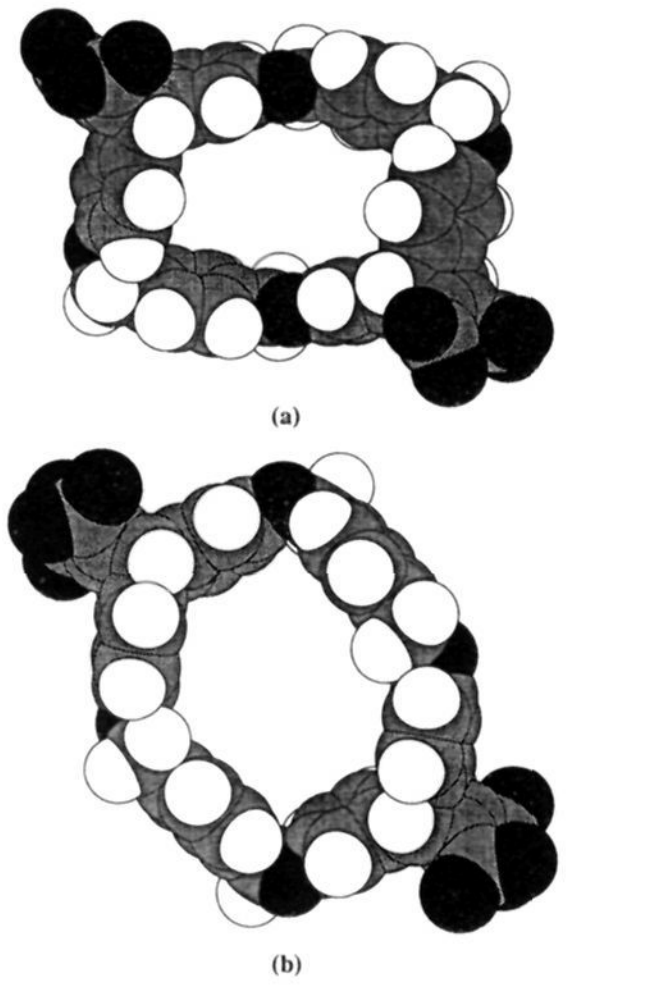

Figure 5. Host $\mathbf{1_S}$ in rhomboid (a) and toroid (b) binding conformations. The rhomboid represents the conformation of the crystal structure of **1**-tetramethyl ester, while the toroid is a calculated conformation.

CD studies of other hosts derived from **1** have also shown the rhomboid vs toroid binding conformations with appropriate guests.[39]

Induced Circular Dichroism in Chromophoric Guests

Induction of circular dichroism in an achiral chromophore by complexation to a chiral receptor is well-known from studies of cyclodextrins[14-16] and some biological molecules.[40] As expected we also see induced circular dichroism (ICD) in our host−guest systems. Table 4 gives the experimentally determined optical constants and rotational strengths for the complexes that show induced CD. In absolute magnitude, the ICDs seen in these systems are generally larger than those seen in cyclodextrins and other host−guest systems.[14-16,20-21] We attribute this to the stronger interactions between chromophores of host and guest expected for our system.

With the exception of guest **21**, the ICD data with host **1** did not appear very informative for the determination of orientations of bound guests, as the ICD generally showed the same sign with all guests ($\Delta\epsilon < 0$ with $\mathbf{1_S}$, $\Delta\epsilon > 0$ with $\mathbf{1_R}$). But experiments with host **2** (which we believe exhibits guest binding orientations nearly identical to those of host **1**) revealed some interesting differences from host **1**. Guests **30**, **31**, and **32** exhibit opposite signs of ICD with **1** and **2**, while **20** shows the same sign of ICD with **1** and **2**. These discrepancies provided the impetus for the calculations described in the next section.

Calculation of Binding Orientations

In highly chromophoric systems like our hosts, optical activity arises predominately through the coupled-oscillator mechanism (dipolar coupling).[24] The theoretical rotational strength from dipolar coupling is given by eq 6.[24c]

$$R_D = \frac{-2\pi}{hc} \sum_{b \neq a} \frac{v_a v_b V_{\mathrm{i0a,j0b}} \mathbf{R}_{\mathrm{ji}} \cdot (\mu_{\mathrm{j0a}} \times \mu_{\mathrm{i0a}})}{(v_b^2 - v_a^2)} \tag{6}$$

where R_D = the rotational strength contributed by dipolar coupling (cgs units), $\mathbf{R}_{ij}$ = the interchromophoric distance vector, μ_{i0a} and μ_{j0a} = electronic transition dipole moment vectors, c = speed of light, h = Plancks constant, and $V_{i0a,j0b}$ is the interaction potential between the two transitions using the point dipole approximation. It is defined by eq 7

$$V_{\mathrm{i0a,j0b}} = \frac{\mu_{\mathrm{i0a}} \cdot \mu_{\mathrm{j0b}}}{\mathrm{R}_{\mathrm{ij}}^3} - \frac{3(\mu_{\mathrm{i0a}} \cdot \mathbf{R}_{\mathrm{ji}})(\mu_{\mathrm{j0b}} \cdot \mathbf{R}_{\mathrm{ji}})}{\mathrm{R}_{\mathrm{ij}}^5} \tag{7}$$

The coupled oscillator approach to calculating ICD (and thus determining binding orientations) has seen much application in studies of cyclodextrin based systems.[15,16] The general approach has been to treat each bond in the host (cyclodextrin) as a chromophore with a single transition moment. Each of these transitions are then coupled with the transition of interest in the guest using a variation of eqs 6 and 7.[15f,16c,41] Our approach to the use of eqs 6 and 7 was to break up the interacting molecules into their component chromophores and use semi-empirical calculations (INDO/S) to determine all the transition moments of each individual chromophore. The individual transition moments can then be superimposed onto the framework of the host−guest system and eqs 6 and 7 used to calculate the ICD of a given guest transition coupled to the host transitions. Although we feel this approach is a more accurate

(39) Ngola, S. M.; Kearney, P. K.; Forman, J. E.; Dougherty, D. A. Unpublished results.

(40) (a) Norden, B.; Kubista, M. *NATO ASI Ser., Ser. C* **1988**, 242, 133−165. (b) Hatano, M. *Induced Circular Dichroism in Biopolymer-Dye Systems*; Springer-Verlag: Berlin, 1986.

(41) Kodaka, M. *J. Am. Chem. Soc.* **1993**, *115*, 3702−3705.

Table 4. Induced Circular Dichroism (ICD) Observed in Aqueous Borate Buffer

guest	host	λ_{max} free guest (nm)	λ_{max} for induced CD (nm)	$\Delta\epsilon$ (L/mol cm)	rotational strength (cgs)
11	$\mathbf{2_R}$[a]	318	315	+14.6	$+2.6 \times 10^{-39}$
20	$\mathbf{1_S}$	355	357	−8.0	-2.2×10^{-39}
21[b]	$\mathbf{2_R}$	355	356	$\Delta\epsilon > 0$	$R > 0$
			341	+1.5	$+9.1 \times 10^{-41}$
21	$\mathbf{1_R}$[c]	323[d]	309	−8.8	-1.1×10^{-39}
24	$\mathbf{1_R}$	570	ICD not obsd[d]	N/A[e]	N/A[e]
		337	340	+0.74	$+1.5 \times 10^{-40}$
24[b]	$\mathbf{2_R}$	570	ICD not obsd[d]	N/A[d]	N/A[d]
		337	321	$\Delta\epsilon > 0$	$R > 0$
25	$\mathbf{1_S}$	467	ICD not obsd[d]	N/A[d]	N/A[d]
		376	379	−5.6	-1.5×10^{-39}
		292	299	shows excitonic coupling with host transition	negative excitonic chirality
		467	ICD not obsd[d]	N/A[d]	N/A[d]
25[b]	$\mathbf{2_R}$	376	379	$\Delta\epsilon > 0$	$R > 0$
		292	297	shows excitonic coupling with host transition	positive excitonic chirality
28[b]	$\mathbf{2_R}$[a]	366	376	$\Delta\epsilon > 0$	$R > 0$
30	$\mathbf{1_S}$	452	456	−4.7	-3.5×10^{-39}
30[b]	$\mathbf{2_R}$	452	470	$\Delta\epsilon < 0$	$R < 0$
31	$\mathbf{1_S}$	439	455	−3.1	-7.4×10^{-39}
31[b]	$\mathbf{2_R}$	439	470	$\Delta\epsilon < 0$	$R < 0$
31	$\mathbf{3_S}$	439	ca. 450	$\Delta\epsilon < 0$[f]	$R < 0$[f]
32	$\mathbf{1_S}$	412	422	−18.8	-3.5×10^{-39}
32[b]	$\mathbf{2_R}$	412	427	$\Delta\epsilon < 0$	$R < 0$
32	$\mathbf{3_R}$	412	448	−3.4	-7.4×10^{-40}
35	$\mathbf{3_S}$	424[g]	439	−145	-1.5×10^{-38}
			419	+15.6	$+2.0 \times 10^{-40}$
35	$\mathbf{4_R}$	424[g]	1:1 complex 447	−18[h]	-1×10^{-38}[h]
			429	+7[h]	$+5 \times 10^{-40}$[h]
			1:2 complex 438	+96[h]	$+7 \times 10^{-39}$[h]
			419	−71[h]	-9×10^{-39}[h]
36	$\mathbf{3_S}$	414	418	−38.9	-2.5×10^{-39}
36	$\mathbf{4_R}$	414	421	+153	$+9.2 \times 10^{-39}$

[a] No ICD was detectable for this guest with host **1**. [b] A binding constant was not obtained for this host−guest system. ICD is from qualitative control study. [c] No ICD was detectable for this guest with host **2**. [d] The data come from the observed UV band of free guest; unfortunately the band was too broad to pick out the true λ_{max} for both of the transitions. [e] While it is tempting to assume this transition has $\Delta\epsilon \approx 0$ and $R \approx 0$, it should be noted that the ICD may have been undetectable under the conditions of our studies. [f] Consistent data is only obtained when [**3**] > [**31**], under conditions of excess guest there is evidence for the formation of complexes of the general form HG_n where $n \geq 2$. ICD data for this guest was very noisy and thus not quantifiable. [g] Soret band of porphyrin, ICD resolves it into the two component bands. [h] Given the inaccuracy in the binding constants for this host−guest system (see discussion), the values given here are approximate.

Chart 2. Binding Constants ($-\Delta G°$, kcal/mol) for Guests Bound by Host **3** in Aqueous Borate Buffer (pH 9) Measured by CD

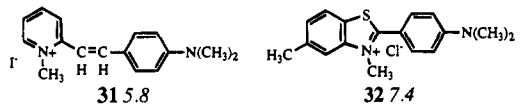

31 *5.8* **32** *7.4*

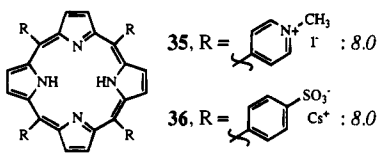

Chart 3. Binding Constants ($-\Delta G°_a$, kcal/mol) for Guests Bound by Host **4** in Aqueous Borate Buffer (pH 9) Measured by CD

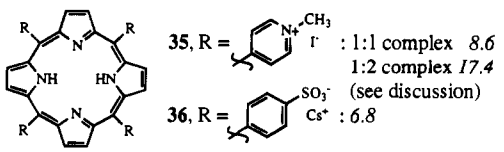

approximation of ICD data, our goal was to obtain qualitative rather than quantitative agreement of calculation with experimental data.

Host **1** can be thought of as being made up of four independent chromophores; the two *p*-xylyl linkers and the two ethenoanthracene units. While the average conformation of the individual chromophores should be the same for each set (linkers and ethenoanthracenes) based on C_2-symmetry in the host rhomboid binding conformation, the crystal structure of $\mathbf{1_S}$ tetramethyl ester shows slight asymmetry between the two units of each set. We felt that this asymmetry might also be typical of the host in solution, and so the calculations were carried out using the four distinct chromophores implied by the crystal structure. This slight degree of asymmetry between what should be equivalent chromophores, however, produced only very small perturbations in the calculated transitions of the chromophores. Semiempirical methods do not lend themselves to the calculation of anionic species with high accuracy, so we approximated the host as the tetraacid (as opposed to tetracarboxylate). Experimental data show that the tetraester and tetraacid of host **1** and related structures have nearly identical CD and UV spectra.[43] Thus we felt that using the crystal structure of our tetraester with replacement of esters by acids was justifiable. In addition, INDO/S calculations are expected to be reliable only for $\pi \rightarrow \pi^*$ transitions, so only states predominated by $\pi \rightarrow \pi^*$ contributions were considered. This exclusion of states predominated by $n \rightarrow \pi^*$ and $\sigma \rightarrow \pi^*$ is not expected to affect the reliability of the calculations, as the low oscillator strengths of

(42) Forman, J. E.; Dougherty, D. A. Unpublished results.

(43) It is important to note that many of the experimental hosts were of "*R*" stereochemistry (Table 4), while the calculations were performed on hosts of "*S*" stereochemistry. When such a discrepancy exists, the calculations are interpreted based on the opposite sign of the data in Table 4.

Chart 4. Calculated Transition Moments for Guests with Observable Induced Circular Dichroism

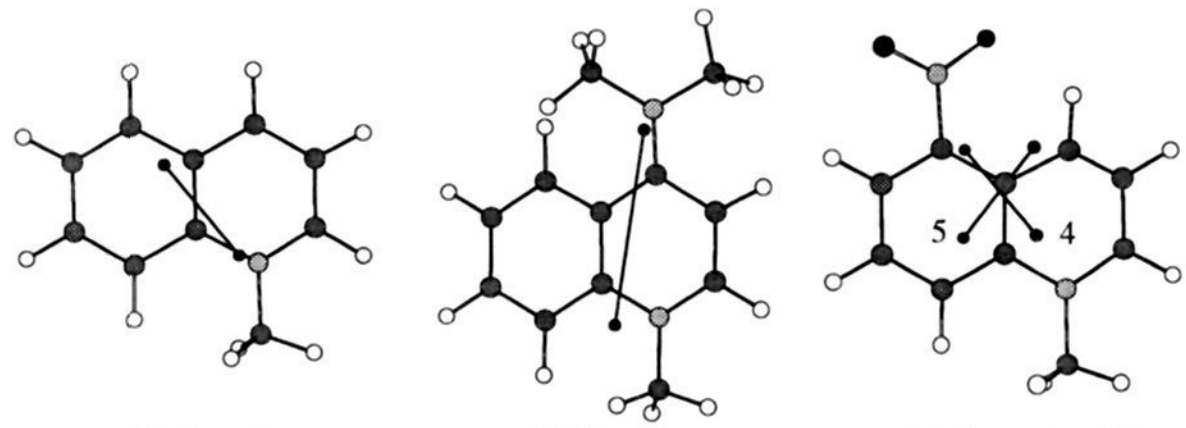

11, State 2 **20**, State 2 **21**, States 4 and 5

24, States 2 and 3 **25**, States 2 and 5 **25**, State 6

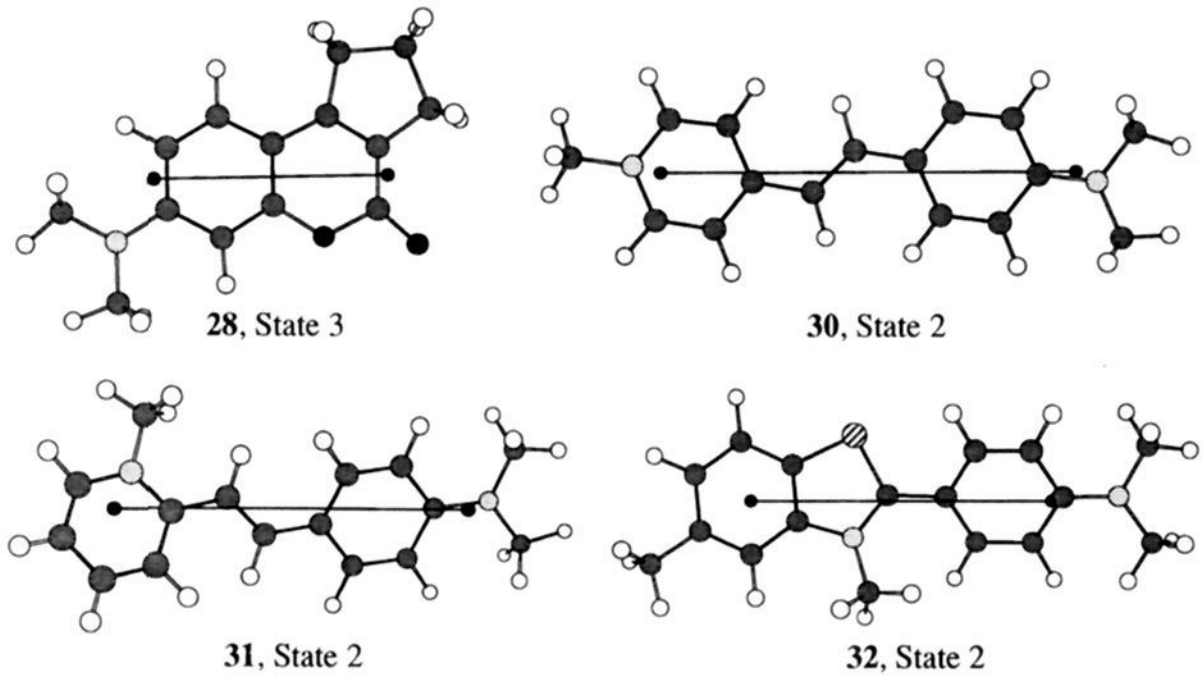

28, State 3 **30**, State 2

31, State 2 **32**, State 2

these transitions should not significantly contribute to calculated rotational strengths. An additional constraint of the calculations was the limitation of transitions to only those above 180 nm (the energy gap between shorter wavelength host transitions and longer wavelength guest transitions results in insignificant contributions to the rotational strength of the induced transition). Comparison of the calculated wavelengths for the transitions with actual spectra showed good agreement in general, so for purposes of the calculations the calculated wavelengths were not corrected to approximate experimental observations. INDO/S transitions were calculated for the guests using AM1 optimized geometries. The *trans*-isomer of **31** was assumed for all calculations involving this guest, and all calculations used the $\mathbf{1}_S$ and $\mathbf{2}_S$ host stereochemistries.[43] Full listings of all calculated transitions, oscillator strengths, and transition dipole moment vectors are provided as supporting information. The important guest transition dipole moment vectors are illustrated in Chart 4.

We set the origin of our coordinate system as the center of mass of the six aromatic rings that form the host cavity. The z-axis is defined as the axis coming directly out of the cavity, and we define the angle θ as the angle of inclination with respect to the z-axis (Figure 6). A general orientation of a transition moment in the xz-plane (as defined in Figure 6) will have θ varied from 0° (aligned on z-axis) through 360° by rotation of the transition moment counter clockwise about the y-axis.

In the calculations described here, guests were oriented in the cavity based on reasonable binding geometries (specific to the type of guest) and rotated about the y-axis in 10° increments. Unless otherwise specified, the initial orientation ($\theta = 0°$) was alignment of the transition dipole under consideration with the z-axis. Rotational strength (R) was calculated at each 10° increment. The value of R was calculated for the given orientation of the transition moment and was not modified for "impossible" orientations, i.e., guest atoms and host atoms sitting at the same locations in space. Calculation of ICD with host $\mathbf{2}_S$ was done analogously to the case of host $\mathbf{1}_S$, but the linkers were neglected from the coupling.[44]

Long Axis Dyes

Guests **30**, **31**, and **32** can be thought of as "control molecules". CPK and molecular mechanics calculations show that these guests can only orient themselves in the host cavity

(44) In creating the host **2** coordinate system, the linkers of host **1** were converted to cyclohexyl groups and the geometry was optimized without allowing any nonlinker atoms to change position. Thus an identical coordinate system was employed.

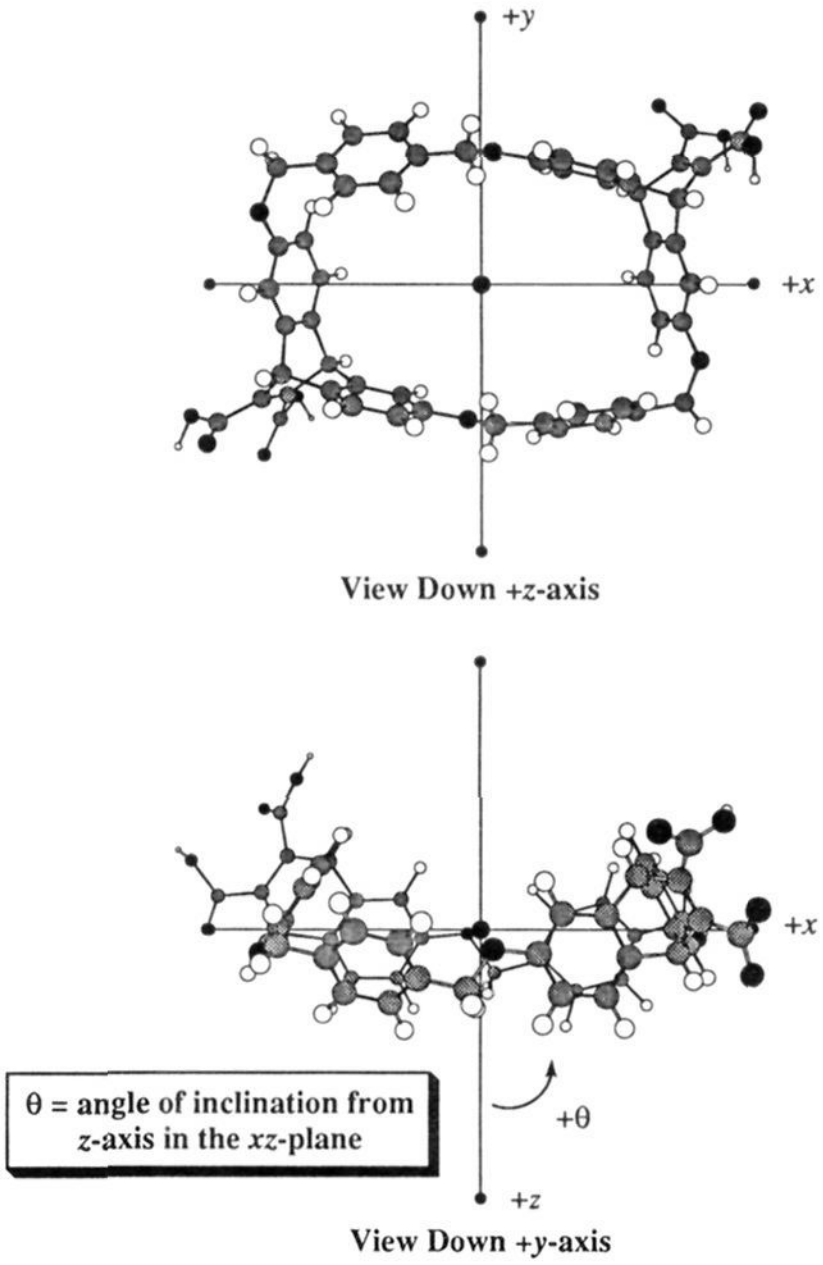

Figure 6. Coordinate system for host $\mathbf{1_S}$. The origin lies at the center of mass of the six aromatic rings that line the cavity.

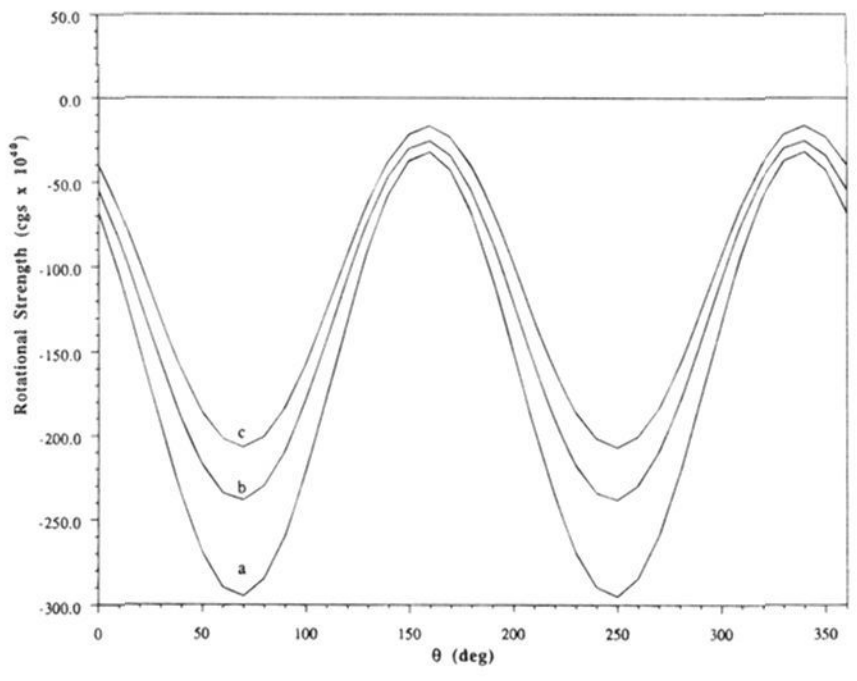

Figure 7. Rotation of guest state 2 transition moments around y-axis. For (a) **30**, (b) **31**, and (c) **32** bound by host $\mathbf{1_S}$.

with the long axis less than 90° (and probably much less than 90°) inclined from the z-axis in the xz-plane. For purposes of calculation, the starting orientation put the guest long axis transition moment in the xz-plane, aligned along the z-axis with the midpoint of the transition moment coincident with the origin. The ICD vs θ curves are shown in Figures 7 and 8. The host **1** calculations (Figure 7) are relatively uninformative as $R < 0$ for all values of θ, but the host **2** data (Figure 8) confirm what the models have shown. Host $\mathbf{2_S}$ should show induced CD with $R > 0$ for all three of the long axis guests.[45] According to the calculations this puts the transition moments at $140° \leq \theta \leq$

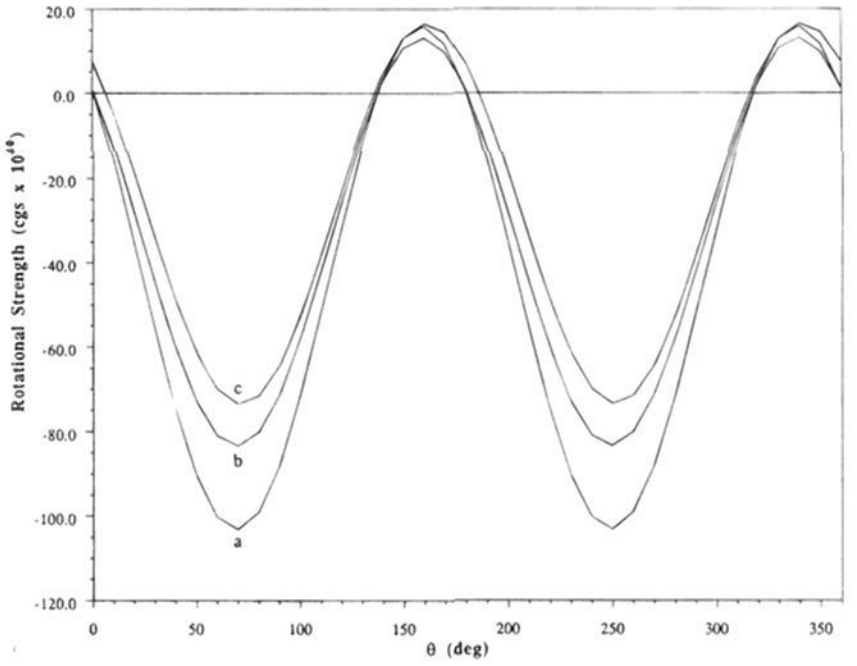

Figure 8. Rotation of guest state 2 transition moments around y-axis for (a) **30**, (b) **31**, and (c) **32** bound by host $\mathbf{2_S}$.

185° (±180°) or up to 40° off perfect alignment with the z-axis for guests **30** and **31**. Guest **32** has a slightly broader range, $135° \leq \theta \leq 190°$ (±180°). Based on the size of the guests, θ approaching 90° should be impossible to attain, and this is confirmed by the calculation. The host **2** cavity is thought to be slightly narrower than host **1**, and so a guest in host **1** may have a slightly broader range of allowed θ's.

The binding orientation suggests that these guests may twist in order to better fill the cavity and to push their aromatic rings into the aromatic cavity walls. In each of the three guests one ring is electron deficient, and we believe that it is the electron poor ring that pushes up to the electron rich face of a cavity aromatic ring. One intriguing aspect of the calculations is the preference for two of four possible binding orientations (Figure 9). The difference in sign of ICD for these seemingly equivalent orientations suggests that the interaction of wave functions of cavity walls and guest differ significantly. The difference is apparently strong enough to result in a preference for a clockwise inclination from the z-axis (Figure 9). AM1 calculations show that guest **30** is ideally planar, but there is a low energy barrier to conformations in which the aromatic rings are twisted relative to the plane of the ethylene bridge;[46] guests **31** and **32** are twisted in their ideal conformations (AM1 calculations). We propose that the chirality of the host induces a subtle preference for the rings of guests **30**, **31**, and **32** to be twisted to cause a better fit (and thus better cation-π stabilization) at one side of the cavity.[47] These data suggest that there is some directionality in the cation-π effect acting as a stabilizing force in molecular recognition.

Azulenes

Guests **24** and **25** were chosen for study because each has a pair of well-defined, mutually perpendicular long wavelength transition moments (oriented along the long and short axes of the molecule, see Chart 4). It was also of interest to determine if a cation-π effect is operative with the seven-membered "cationic" ring of the guest.[12a,33] As with the long axis guests, the starting orientation put the guest transition moment in the xz-plane, aligned along the z-axis with the midpoint of the transition moment coincident with the origin.

(45) Experimentally, host $\mathbf{2_R}$ shows induced CD with $R < 0$ for these guests.

(46) Ponterini, G.; Momicchioli, F. *Chem. Phys.* **1991**, *151*, 111−126.

(47) Similarly, a recent molecular dynamics study on host **1** with acetylcholine (**17**) as guest showed that the guest prefers to reside at one side of the cavity. Axelson, P. H. *Isr. J. Chem.* **1994**, *34*, 159−163.

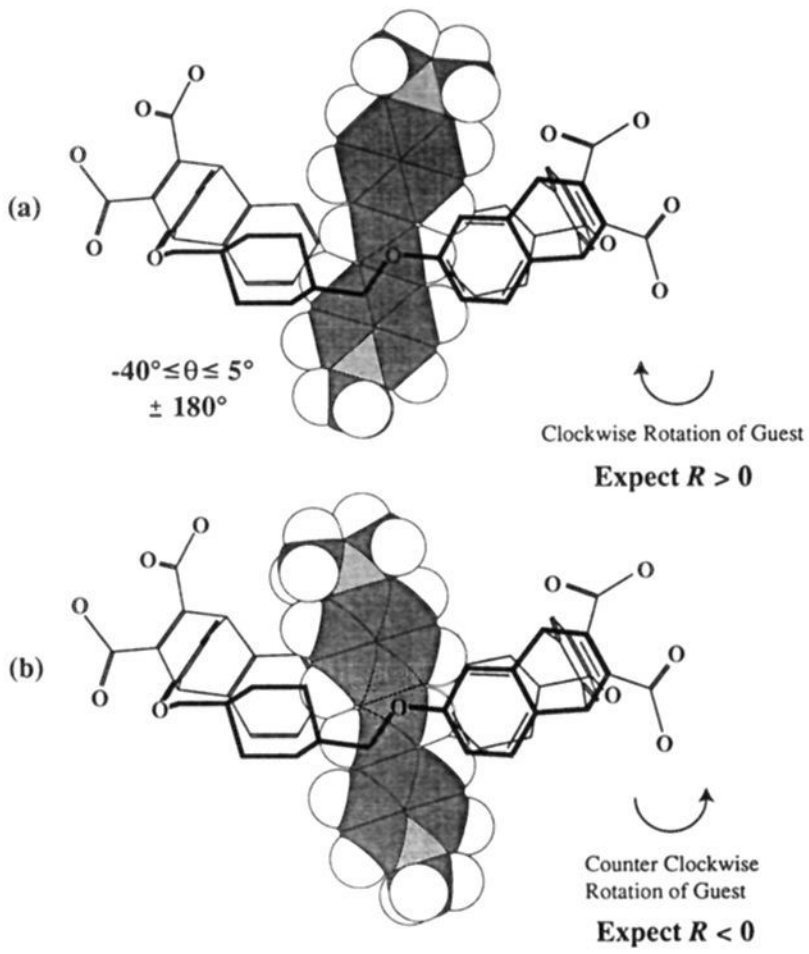

Figure 9. Observed (a) and non-observed (b) binding orientations for long-axis guests with host $\mathbf{2_S}$ (illustrated with guest **30**). View is down $+y$-axis, and the guest lies in the xz-plane and is positioned with the long-axis transition moment at an angle midway through the range of allowed θ's off the z-axis. Note that each of the two orientations shown has generates an equivalent orientation by adding 180° to the value of θ.

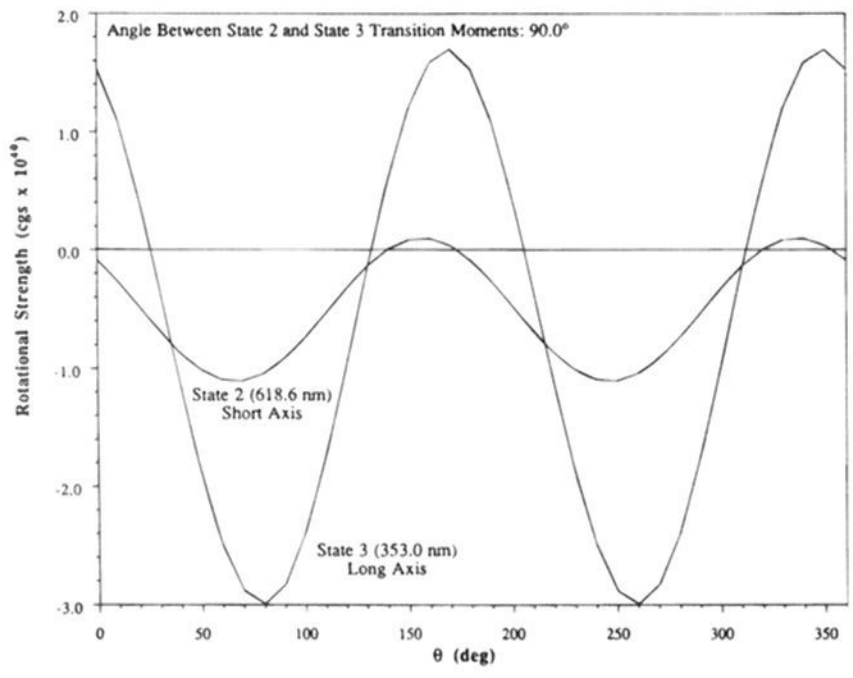

Figure 10. Rotation of guest transition moment around y-axis for azulene (guest **24**) bound by host $\mathbf{2_S}$.

Figure 10 shows the expected rotational strength for bound conformations of azulene (**24**) with host **2**. Only the transition to state 3 was experimentally observed (with both hosts **1** and **2**), this transition being polarized along the long axis of the guest (Chart 4). The expected $R < 0$ (Table 4) places the binding orientation from 30°−130°(±180°). A similar calculation with host **1** places the binding orientation from 0°−140°. This suggests the guest is most likely to be near the 90° orientation. That is, the guest prefers to be nearly fully encapsulated in the host—a binding conformation consistent with a strong hydrophobic effect contributing to the binding. Models show that the host cavity is long enough to accommodate the long axis. We were unable to experimentally see ICD for state 2 (short axis transition, 90° inclination from state 3). The

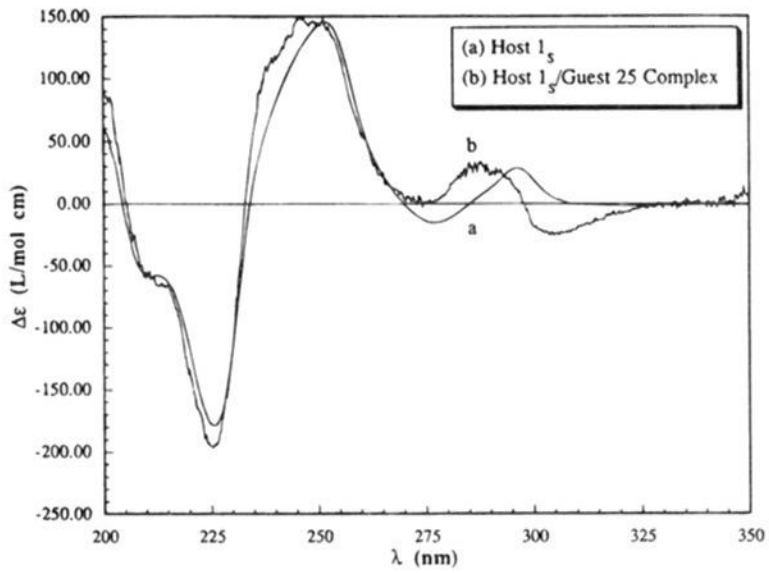

Figure 11. Best fit CD spectra of host $\mathbf{1_S}$ and its complex with guest **25** in aqueous borate buffer (pH 9).

calculations do indicate that, generally, the magnitude of $\Delta\epsilon$ should be smaller for state 2 than for state 3. If we assume our observation is not an experimental artifact but rather indicates that $\Delta\epsilon \approx 0$, Figure 10 suggests the binding orientations for host **2** to be in the range of 140°−175°(±180°). This would imply 50−85°(±180°) for state 3, a result consistent with the direct analysis of state 3. Again, host **1** is expected to have a similar binding orientation.

A similar result is seen with guest **25**, with state 2 ICD predicted to be *very* weak in intensity. Analysis of the state 5 (long-axis) transition again predicts that the long axis prefers to be enclosed in the host cavity. Guest **25** also shows an interesting spectral feature in its host−guest complex with both hosts **1** and **2** (data for host **1** shown in Figure 11). It appears that the transition to state 6 (short axis, near 300 nm) shows an excitonic coupling[25] (split Cotton effect centered near 300 nm) to state 5 of the ethenoanthracene chromophores of the host. Using the general equation for excitonic coupling,[25] the expected signs of the excitonic chirality for the host **1/2**−guest **25** complexes were computed. Based on the observed negative chirality for $\mathbf{1_S}$ (negative first Cotton effect, positive second Cotton effect), the calculation gives a short axis binding orientation in the range 120°−240°(±180°). This corresponds to 40°−150°(±180°) for the guest long axis. While broad, the range of θ is completely consistent with the data obtained from direct analysis of ICD curves for **24** and **25**, ruling out the orientation where the seven-membered "cationic" ring is exclusively bound (0° with respect to long axis of guest).

Quinolines and Coumarins

Guests **11**, **20**, and **21** were oriented in the xz-plane so that the C(9)−C(10) bond of the quinoline ring was coincident with the z-axis, and the midpoint of this bond was placed at the origin. The midpoints of the C(2)−C(3) and C(6)−C(7) bonds were bisected by the x-axis. Starting with this orientation, the guest was rotated about the y-axis to give the R vs θ curves. Unlike the previous guests, whose orientations were determined by the transition moments, the three quinolines each have two initial orientations that need to be considered (Figure 12).

Experimentally guest **11** only shows ICD with host **2**. In the case of host **1** the ICD band is thought to be buried under the tail of the host longer wavelength Cotton effects. Figure 13 shows the expected rotational strength for guest **11** interacting with host **2**. The data ($\mathbf{2_S}$, $R < 0$) puts θ at 0°−100°(±180°) for orientation #1 and 80°−185°(±180°) for orientation #2. In each case the guest appears to rotate in such a way as to place the *N*-methyl group into the cavity (Figure 14). Since the methyl group carries a large fraction of the positive charge in such a

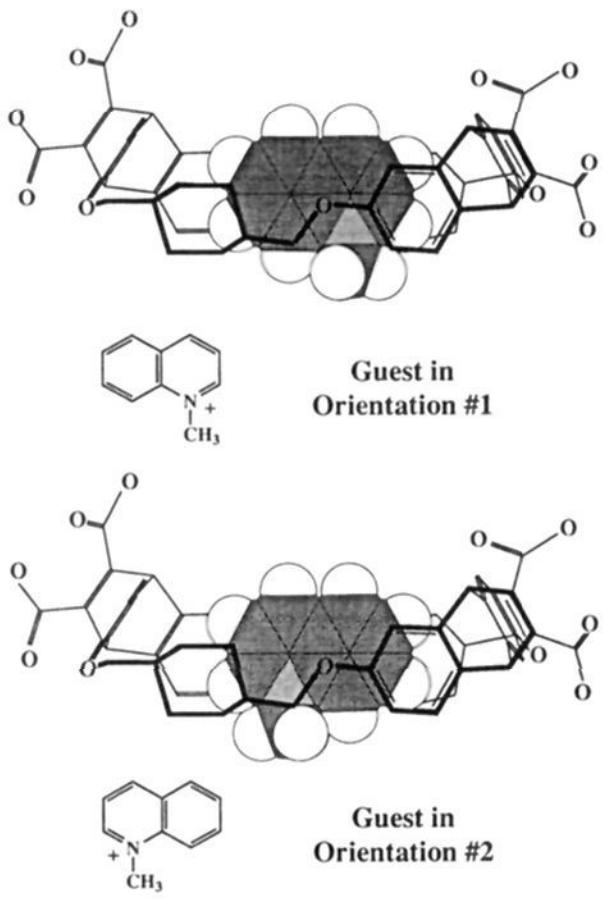

Figure 12. $\theta = 0°$ orientations for *N*-methylquinolinium (**11**) derived guests. The quinoline ring lies in the *xz*-plane of the host coordinate system (Figure 6). The view here is down the $+y$-axis (illustrated with host $\mathbf{2_S}$).

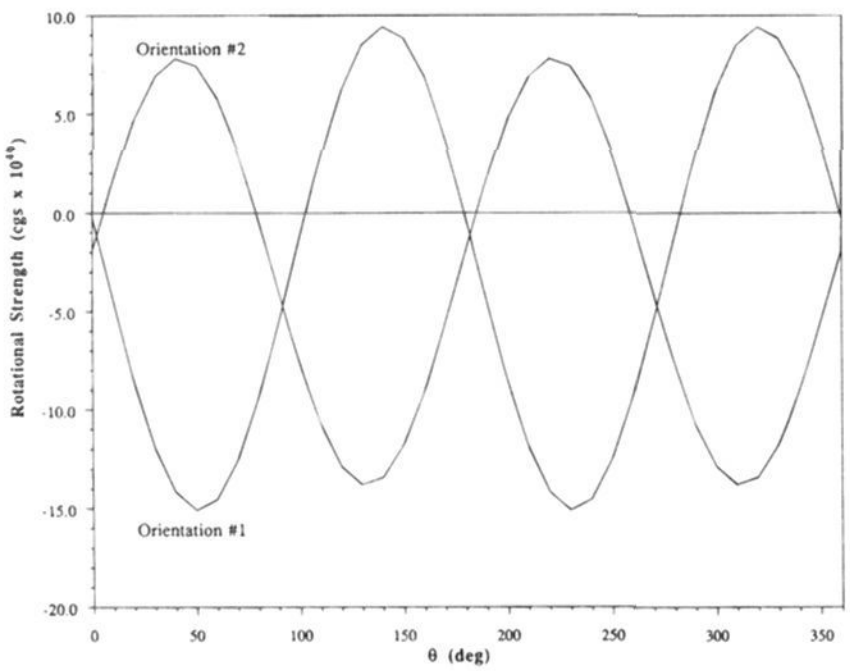

Figure 13. Induced CD expected for binding orientations obtained by rotation of guest central bond around *y*-axis for guest **11** bound by host $\mathbf{2_S}$.

structure, this finding is consistent with the cation-π interaction influencing binding orientations.

NMR experiments with guest **11** and host **1** show that the protons in the 2, 6, and 7 positions on the quinoline ring experience greater upfield shifting on complexation than do other guest protons.[48] We believe that these protons are therefore more deeply buried in the host cavity than are the remaining (more exposed) guest protons. The binding orientations shown in Figure 14 are consistent with these NMR observations. In particular the proton at the 2-position is shown to be near the cavity walls in all four of the Figure 14 binding orientations, and this proton is upfield shifted to the greatest extent in the NMR studies.[48] As expected we observe binding orientations for host **1** that are similar to those of host **2** with a given guest.

Similar calcuations were performed for guest **20**. With host $\mathbf{1_S}$ ($R < 0$, Table 4), the data puts θ at $10°-140°(\pm180°)$ for orientation #1 and at $-25°-125°(\pm180°)$ for orientation #2. The host **2** data narrows the range of θ giving ranges of $35°-125°(\pm180°)$ for orientation #1 and $30°-115°(\pm180°)$ for orientation #2 (where $\mathbf{2_S}$ is expected to produce $R < 0$). Again the data for the two systems are consistent and indicate that the guest rotates in such a way as to place one substituent inside the cavity. In this case there are two substituents, the *N*-methyl and 4-dimethylamino groups. We expect the preferred orientation would place the hydrophilic dimethylamino group exposed to solvent and the hydrophobic methyl group in the cavity (Figure 15). This also puts the formal positive charge in the cavity where it can experience cation-π interactions.

For guest **21**, induced CD was observed only with host $\mathbf{1_S}$. The expected rotational strength is shown in Figure 16. This guest was of particular interest as the ICD was observed for two nearly in plane transitions separated through an angle of 83.5° (states 4 and 5, see Chart 4). The θ range satisfying the observed ICD (state 4 $R > 0$, state 5 $R < 0$) for host $\mathbf{1_S}$ is $80°-150°(\pm180°)$ for orientation #1 and $0°-70°(\pm180°)$ for orientation #2. This indicates a preference for binding orientations in which both substituents are outside the cavity (Figure 17). This places the relatively hydrophilic nitro group in a relatively solvent exposed environment. This result is in contrast to the preferred orientations of guests **9** and **20** where a substituent is pushed into the cavity. It may be that a 1,5 substitution pattern does not allow a comfortable fit in the cavity unless both substituents are outside.

The coumarin dyes **26**−**29** did not show detectable ICD with host **1**, and only **28** gave detectable ICD with host **2**. Calculation by orienting the guest with its transition moment coincident with the *z*-axis and the midpoint of the transition moment at the origin, places θ in the range $30°-130°(\pm180°)$ for $R<0$ with host $\mathbf{2_S}$. As seen with guests **24** and **25**, this puts the guest in an orientation that allows most of its surface area to be placed in the cavity. The data suggests hydrophobic forces dominate the binding of this guest.

Larger Hosts (3 and 4)

Binding Conformations. CD studies with hosts **3** and **4** generally show rhomboid-like changes on binding guests, but there is some evidence for a toroid-like conformation with **3**.[49] There is a general decrease in binding affinity on moving from **1** to the less conformationally restricted **3** and **4**. Both **3** and **4** are expected to exist in aqueous solution as highly collapsed structures. Also in both **3** and **4** the ethenoanthracene units can twist so that the carboxylates can enter the cavity, thus allowing electrostatic contributions to the binding that are much stronger than in host **1**. This enhancement of electrostatic contributions to binding is thought to be more significant for **4** and is probably important in the binding of positively charged guests such as **35**.

ICD and Other Spectral Changes Associated with Guest Binding. As with **1** and **2**, some guests show bathochromic shifting on binding to **3** and **4**. Red shifting for guests **31** and **32** with **3** reveal an inconsistent relationship compared with **1** and **2** (smaller shift with **31**, larger shift with **32**). This is thought to be the result of significantly different binding conformations. In support of this claim the two guests exhibit

(48) The extent of upfield shifting of ^{1}H NMR peaks (*D* values) for all of the protons of guest **11** relative to one another, are as follows: methyl 0.69, 2-position 1.00, 3-position 0.27, 4-position 0.69, 5-position 0.69, 6-position 0.96, 7-position 0.84, and 8-position 0.65. Kearney, P. C. California Institute of Technology, Ph.D. Thesis, 1994.

(49) This is observed in the encapsulation of large cations such as $Ru(phen)_3^{2+}$. Forman, J. E.; Dougherty, D. A. Unpublished results.

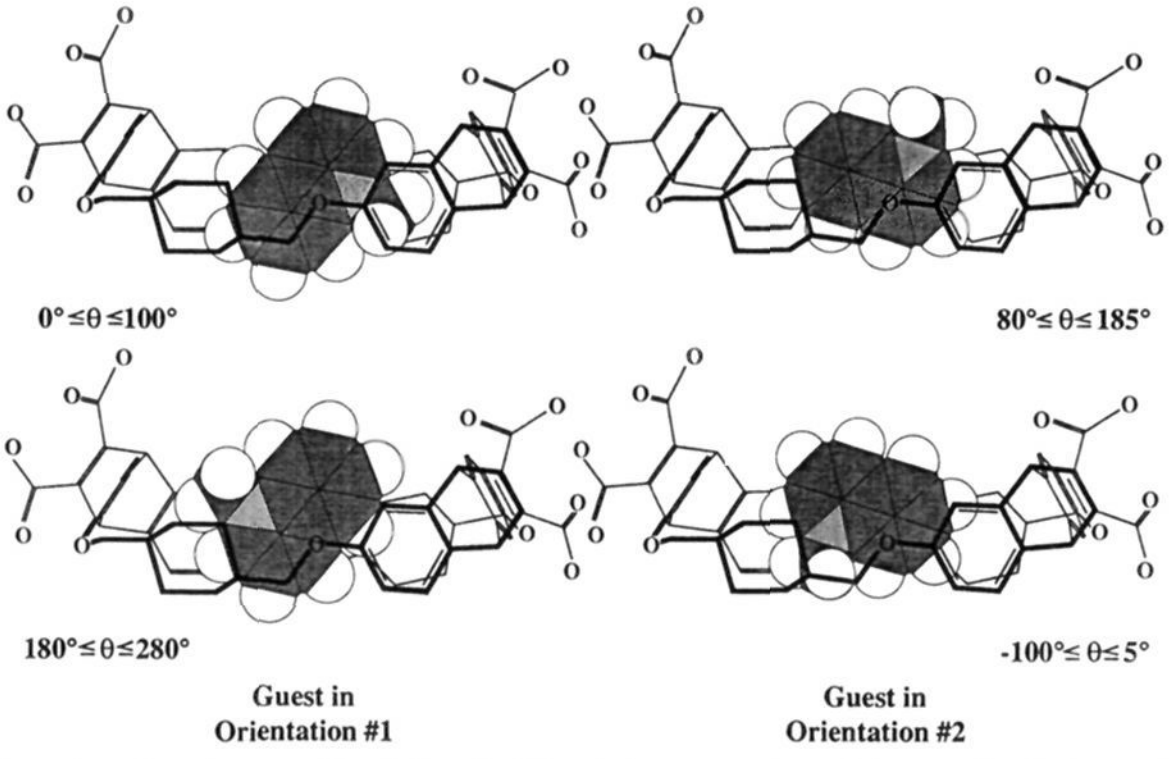

Figure 14. Possible binding orientations for guest **11** with host $\mathbf{2_S}$. View is down $+y$-axis, and the guest lies in the xz-plane and is positioned with the C(9)−C(10) bond at an angle midway through the range of allowed θ's off the z-axis.

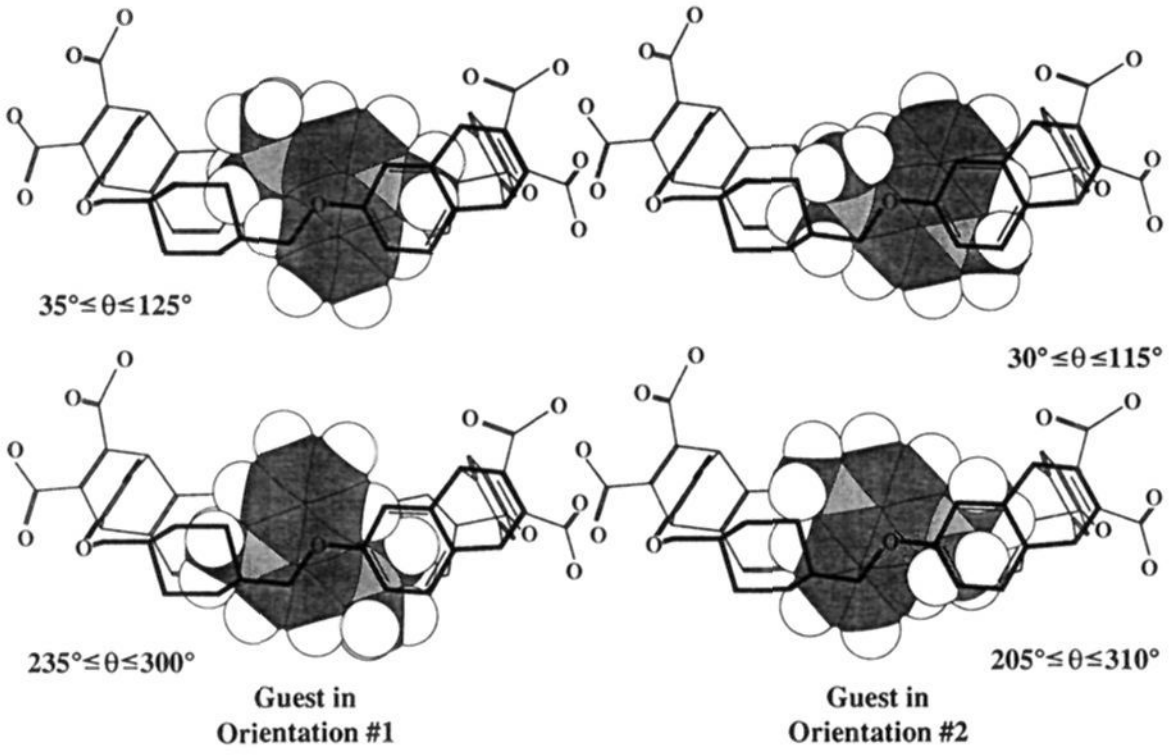

Figure 15. Possible binding orientations for guest **20** bound by host-$\mathbf{2_S}$. View is down $+y$-axis, the guest lies in the xz-plane and is positioned with the C(9)−C(10) bond at an angle midway through the range of allowed θ's off the z-axis.

opposite signs for their respective ICD (both guests have long axis transition moments). In addition, we observe sign reversals in the ICD of **31** when binding studies are carried out with excess guest. Such spectral changes are thought to be the result of additional guest molecules entering the cavity to produce HG_2 and/or higher order complexes. Guest **22** with host **3** does not show this behavior.

As might be expected, some guests show 2:1 and/or higher order complex formation with these larger hosts. The most notable examples are the **3/31** and **4/35** systems. For the other host−guest systems (**3/32**; **3/35**; **3/36**; and **4/36**) control studies with excess host reveal no unusual spectral changes—these complexes are thought to be exclusively 1:1 guest−host.

The dipolar coupling mechanism of ICD[24] is evident in examination of the rotational strengths in Table 4. In general **3** induces greater rotational strengths than **1**, and **4** induces greater rotational strengths than **3**. This is expected from the coupling of a greater number of host transitions with the guest transition in the higher oligomers. Unfortunately, no rigorous conformational data are available for **3** and **4**, so induced CD calculations were not attempted for these hosts and their guests.

Porphyrins as Guests. The tetracationic porphyrin **35** shows significant CD changes on binding to **3** and **4**. For the **3/35** system a strong Cotton effect is observed at 439 nm (red shifted 15 nm from the UV Soret λ_{max}), and a weaker Cotton effect is observed at 419 nm (5 nm blue shift from UV Soret λ_{max}). We believe this results from induced CD in the two mutually perpendicular component transitions in the Soret band (the long wavelength B_x transition lies along a line connecting the H atoms of opposing pyrrole groups). This observation of a split Cotton effect in induced CD for **35** has been observed in the intercalation of helical peptides and polymers.[50] In the case of the **3/35** complex, the two Cotton effects are not equivalent in rotational strength. Guest **36** also does not show the split induced CD for the Soret bands with either host **3** or **4**. We believe these observations to be the result of a much less specific binding orientation, where all guest orientations average to give a single induced CD band. The single induced CD band could also result from the host causing the porphyrin ring to bend out of the plane.

With the **4/35** system two distinct spectral patterns are observed, depending on whether one is under conditions of

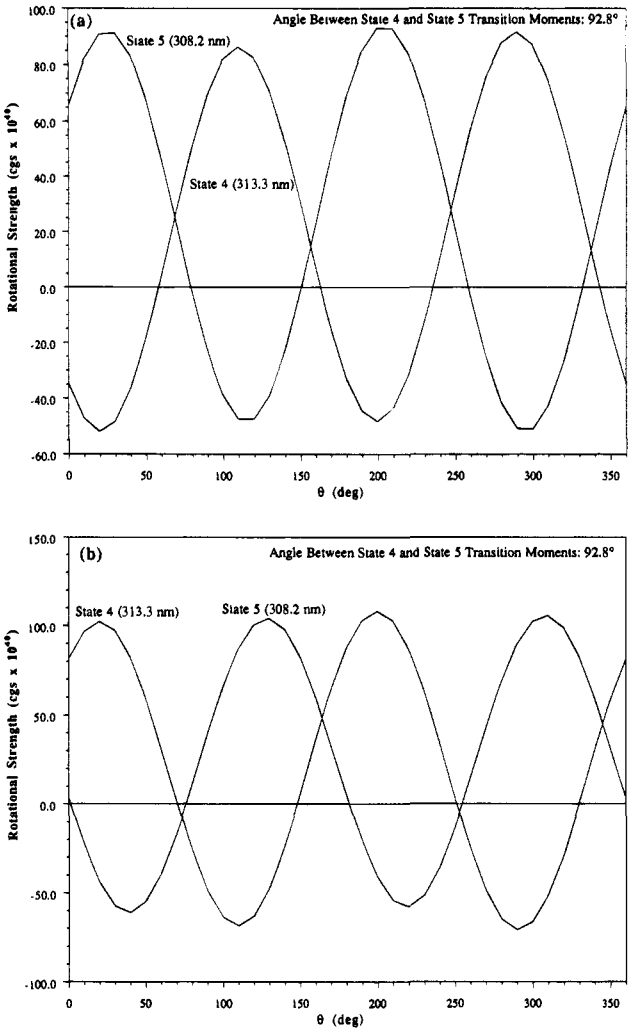

Figure 16. Induced CD expected for bound guest in orientation obtained by rotation of guest central bond around *y*-axis for guest **21** with host $\mathbf{1_S}$ (a) guest in orientation #1 and (b) guest in orientation #2.

excess host or excess guest (Figure 18). In the case of excess host, the expected split Cotton effect is observed as with **3**, but the rotational strengths of the two bands are more equally matched. Under conditions of excess guest, the Cotton effect changes sign and is blue shifted relative to the excess host induced CD bands. Mol ratio and Job plots of this data suggest a 2:1 guest–host complex is forming. The discrete signals between 1:1 and 1:2 complexes suggest a specific orientation for the porphyrins in the cavity of **4**.

The binding constants given for this system in Chart 3 are only approximate. The 1:1 number comes from data fitting a series of solutions in which only the spectral features of curve a in Figure 18 were evident. Starting from the 1:1 complex data and assuming all host was initially present as the complex, a series of solutions for which the spectral features of curve b were evident was fitted assuming formation of a 2:1 complex. The fitting gave $-\Delta G^\circ = 8.8$ kcal/mol for the second association. This gives an overall formation constant of 17.4 kcal/mol for the 2:1 complex. Given the approximations involved in the analysis, however, these values should be considered as only estimates.

It should be noted that the aggregation state of guest **35** in aqueous solution is not clear. The literature contains several conflicting reports in regard to this porphyrin, with different authors claiming it exists exclusively as monomer,[51] exclusively as dimer,[52] or as monomer in equilibrium with dimer[53] under the concentration range we studied. CDfit is unable to account for this aggregation, but our data show good agreement with our model. This leads us to believe that the monomer predominates under our experimental conditions. Consideration of a monomer–dimer equilibrium (using a dimerization constant of $K_D = 1 \times 10^5$ M^{-1})[53] and data fitting with the Benesi–Hildebrand method[54] gives $-\Delta G^\circ = 6.9$ kcal/mol for **3/35**. Benesi–Hildebrand treatment of data without accounting for the monomer–dimer equilibrium gives a value of 7.3 kcal/mol. Guest **36** has also been reported to dimerize ($K_D = 6 \times 10^3$ M^{-1}).[53] These observations may result in additional error in the reported binding constants for **35** and **36**.

Like **3/36** the **4/36** system shows only a single induced CD band. With **36** host **4** is certainly capable of binding two guests (as per guest **37**), but electrostatic repulsions from the high number of negative charges present in both host and guest are thought to keep the complex at a 1:1 stoichiometry.

Guest **36** is significant because our hosts, as a rule, do not bind anionic species. We rationalize the binding of **36** to host **3** and **4** by a cation-π effect with the electron deficient (positive) face of the porphyrin ring. This binding of the porphyrin, but not the phenylsulfonate substituents, is supported by NMR data in 10% CD_3CN/90% borate-*d* (a solvent that decreases aggregation) involving **3/36**. These studies have shown weak downfield shifting of the phenylsulfonate protons—not the strong upfield shifting expected for encapsulation in an aromatic rich cavity. The interaction of host with the electron deficient region of an anionic guest represents a novel cation-π effect previously unobserved in our studies of this phenomena.

Conclusions

The studies reported here demonstrate the use of CD spectroscopy as a viable method for studying molecular recognition in aqueous media. We have demonstrated the accuracy of the method as compared to NMR studies and shown that the two methods complement one another in allowing a more complete range of $-\Delta G^\circ$ values to be obtained. Induced CD

(50) (a) Bustamonte, C.; Gurrieri, S.; Pasternack, R. F.; Purrello, R.; Rizzarelli, E. *Biopolymer.* **1994**, *34*, 1099–1104. (b) Nezu, T.; Ikeda, S. *Bull. Chem. Soc. Jpn.* **1993**, *66*, 25–31. (c) Nezu, T.; Ikeda, S. *Bull. Chem. Soc. Jpn.* **1993**, *66*, 18–24. (d) Pasternack, R. F.; Bustamante, C.; Collings, P. J.; Giannetto, A.; Gibbs, E. J. J. *J. Am. Chem. Soc.* **1993**, *115*, 5393–5399. (e) Pasternack, R. F.; Gibbs, E. J. *Inorg. Organometal. Polym.* **1993**, *3*, 77–88. (f) Pasternack, R. F.; Giannetto, A.; Pagano, P.; Gibbs, E. J. *J. Am. Chem. Soc.* **1991**, *113*, 7799–7800. (g) Pancoka, P.; Urbanová, M.; Bednárová, L.; Vacek, K.; Paschenko, V. Z.; Vasiliev, S.; Malon, P.; Král, M. *Chem. Phys.* **1990**, *147*, 401–413. (h) Pasternack, R. F.; Brigandi, R. A.; Abrams, M. J.; Williams, A. P.; E. J. *Inorg. Chem.* **1990**, *29*, 4483–4486. (i) Pasternack, R. F.; Gibbs, E. J.; Gaudemer, A.; Bassner, A. A. S.; De Poy, L.; Turner, D. H.; Laplace, A. W. F.; Lansard, M. H.; Merienne, C.; Perrée-Fauvet, M. *J. Am. Chem. Soc.* **1985**, 8179–8186. (j) Pasternack, R. F.; Gibbs, E. J.; Villafranca, J. J. *Biochem.* **1983**, *22*, 2406–2414.

(51) (a) Pasternack, R. F.; Francesconi, L.; Raff, D.; Spiro, E. *Inorg. Chem.* **1973**, *12*, 2606–2611. (b) Pasternack, R. F.; Huber, P. R.; Boyd, P.; Engasser, G.; Francesconi, L.; Gibbs, E.; Fasella, P.; Venturo, C. G.; Hinds, L. deC. *J. Am. Chem. Soc.* **1972**, *94*, 4511–4517. (c) Das, R. R.; Pasternack, R. F.; Plane, R. A. *J. Am. Chem. Soc.* **1970**, *92*, 3312–3316. See also reference 47i.

(52) (a) Kano, K.; Takei, M.; Hashimoto, S. *J. Phys. Chem.* **1990**, *94*, 2181–2187. (b) Kano, K.; Hashimoto, S. *Bull. Chem. Soc. Jpn.* **1990**, *63*, 633–635. (c) Kano, K.; Nakajima, T.; Hashimoto, S. *Bull Chem. Soc. Jpn.* **1987**, *60*, 1281–1287. (d) Kano, K.; Miyake, K.; Uomoto, T.; Sato, T.; Ogawa, T.; Hashimoto, S.*Chem. Lett.* **1983**, 1867–1870.

(53) Kemnitz, K.; Sakaguchi, T. *Chem. Phys. Lett.* **1992**, *196*, 497–503.

(54) Connors, K. A. *Binding Constants*; Wiley: New York, 1987.

(55) Schmidtchen, F. P. *Chem. Ber.* **1980**, *113*, 2175–2182.

(56) Hafnex, K.; Bernhard, C. *Ann.* **1959**, *625*, 108–123.

(57) Version 4.0, Micrsoft Corp., Copyright 1985–1992.

(58) Version 2.3, BioSym Technologies, 1993.

(59) We kindly thank Josef Michl for the use of this semiempirical package.

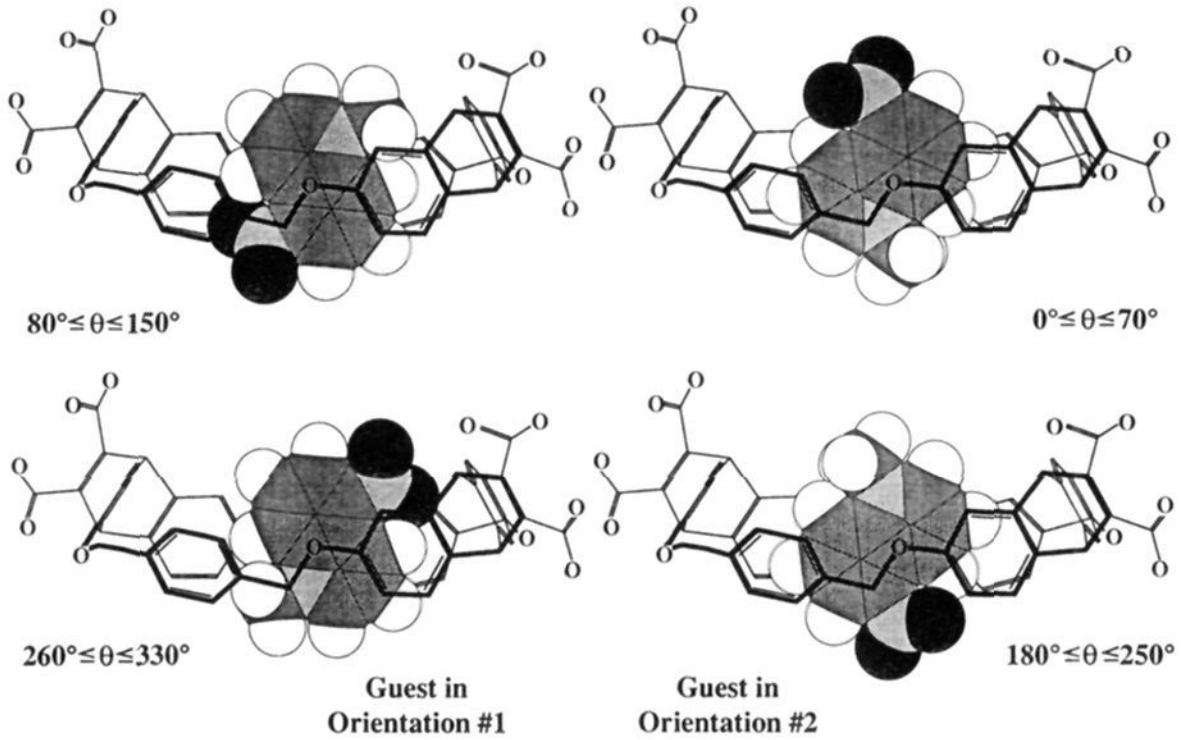

Figure 17. Possible binding orientations for guest **21** bound by host-$\mathbf{1}_S$. View is down $+y$-axis, the guest lies in the xz-plane and is positioned with the C(9)−C(10) bond at an angle midway through the range of allowed θ's off the z-axis.

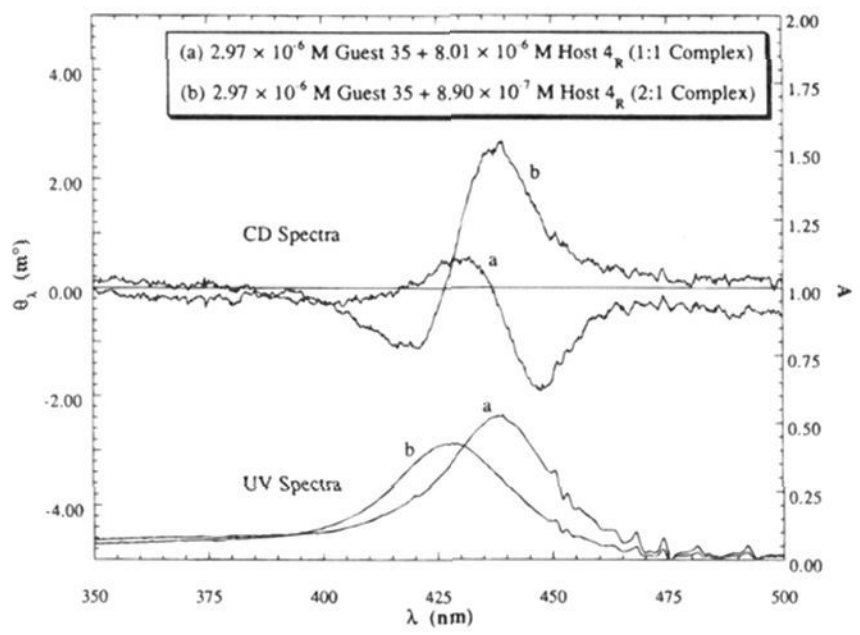

Figure 18. CD and UV spectra of solutions containing guest **35** and host $\mathbf{4}_S$ in aqueous borate buffer (pH 9).

in chromophoric guests has provided evidence of binding orientations, and we have determined these orientations through calculation. The data have revealed a preference of guests to rotate in the cavity to better fill space. CD has also provided experimental confirmation of previously invoked binding conformations. The analytical approaches developed here should be applicable to general studies of molecular recognition and can be modified for use with UV/vis spectroscopy.

The data reported here suggest a directional preference of the cation-π effect for certain orientations of bound guests. Calculated binding orientations for several tightly bound guests indicate a significant hydrophobic contribution to the binding. We have also demonstrated that conformationally unrestrained hosts **3** and **4** can bind guests with high affinity and specific binding orientations. These hosts, although conformationally unrestricted, show significant cation-π effects in guest binding.

Experimental Section

General Methods. CD spectra were recorded on a JASCO J-600 Spectropolarimeter with either 1.0 or 0.5 cm pathlength quartz cells. A standard set of measurement parameters was used in all experiments. UV/vis spectra were recorded on a CARY 2200 or Beckman DU-640 spectrophotometer. IR spectra were recorded on a Perkin-Elmer 1600 FT-IR. GC/MS data was obtained on a Hewlett-Packard 5890/5970 GC/MS. NMR spectra were recorded on a Bruker AM-500 spectrometer; routine spectra were referenced to the residual proton signals of the solvents and are reported in ppm downfield of 0.0 as δ values. NMR spectra in borate-d were referenced to the 1.09 ppm peak of 3,3-dimethylglutarate (DMG) as internal standard. Preparation of solutions used for NMR binding studies and the protocols for such studies have been described previously.[12af,13a]

All solvents used in spectroscopy were spectrophotometric or HPLC grade. Aqueous cesium borate buffer (pH 9) was prepared by dissolving 0.25 g high purity boric oxide in 800 g water and adding 3.74 mL of 1 M CsOH followed by thorough mixing. The water used in these preparations was passed through a Milli-Q purification system.

All reactions, unless otherwise noted, were stirred magnetically under nitrogen atmosphere. Solvents were distilled from drying agents under argon atmosphere: acetonitrile:CaH_2; THF:sodium benzophenone ketyl. Ion exchange for NH_4^+ was carried out with Dowex 50w-x2 cation exchange resin (the resin was treated with concentrated ammonium carbonate then washed with Milli-Q purified water before use). Unless otherwise noted reagents obtained from commercial sources were used without further purification.

Compounds **5**, **6**, **8**, the tetraacids of **1** and **2**, **3** hexamethyl ester, and **4** octamethyl ester were prepared by procedures described previously.[12af]

CD Binding Studies. Solutions of guests were prepared by weighing out solutes on a Sartorius microbalance followed by dilution to appropriate volumes. Further dilutions of stock solutions gave the desired concentrations. For sparingly soluble guests **24**, **25**, **26**, **27**, **28**, and **29** saturated solutions in cesium borate buffer were prepared. Aliquots of these saturated solutions were diluted with acetonitrile, and the concentrations were determined by fitting to UV/vis calibration curves of the guest in mixed acetonitrile/cesium borate solvent systems. Stock solutions of guest were prepared fresh for all studies with the sparingly soluble guests and with guests **17** and **32** (these guests decompose on prolonged standing in cesium borate).

Solutions of hosts were prepared by dissolving lyophilized samples of the appropriate polyacid in cesium borate buffer. Concentrations were determined from CD spectroscopy by fitting to standardized $\Delta\epsilon$ data.

Standardized $\Delta\epsilon$ values for hosts were determined from a series of 5−6 solutions of the appropriate host in the $10^{-7}-10^{-5}$ M concentration range. The data at each wavelength in the 200−350 nm range was fitted to the Beer−Lambert law to give the best fit $\Delta\epsilon$ data used in the binding studies. For hosts **1** and **2** these calibration studies used stock solutions prepared and standardized for NMR studies.

Fitting CD data from acetonitrile solutions of **1** tetraacid to $\Delta\epsilon$ values for the 230−350 nm region of **1** tetramethyl ester in CH_3CN provided estimates of purity of samples of the tetraacid. Calibration studies with **1** stock solutions in cesium borate prepared by weighing out samples of the tetraacid (with "known purity") produced nearly identical $\Delta\epsilon$

values to the studies with NMR standardized stock solutions. This method of $\Delta\epsilon$ determination was used for **1** trimer and tetramer.

In a typical CD binding study, 5−6 spectra of solutions with 1 equiv concentration of one component (usually host) but varying concentration of the other component (usually guest) were used. The spectra and the $\Delta\epsilon$ values of the host were fit to an association constant with the CDfit program. In general host concentrations were kept between 1 and 5 μM for **1** and 0.5−2 μM for **3** and **4**. All cases of guest induced CD in fitted $\Delta\epsilon_{HG}$ spectra were confirmed in solutions where [host]:[guest] ratios were alternately very high and very low (high % bound guest and high % bound host).

A CD binding study was taken to be valid when (1) statistical fitting parameters show strong agreement with our model, (2) the samples used in the experiment cover a reasonable portion of the 20−80% bound range of the more dilute component in the solution, and/or (3) the results are reproducible to $-\Delta G° \pm 0.2$ Kcal/mol. CDfit evaluates the statistical parameters RMS and SSR (for individual samples and for the entire data set); the data output includes $\theta_{c\lambda\ calc}$ and $(\theta_{c\lambda\ calc} - \theta_{c\lambda\ obs})$ for all samples. Control experiments with our "half" and "three-quarters" molecules (**6** and **5**), consistently gave poorly fitting, nonreproducible data sets.

3-Hexaacid. In a 25 mL flask 0.016 g (1.17×10^{-5} mol) of 3-hexamethyl ester was dissolved in 8 mL of THF, followed by addition of 0.057 g (3.79×10^{-4} mol) of cesium hydroxide and 2 mL of water. The mixture was allowed to stir in the dark at room temperature overnight, and the THF was removed by rotary evaporation. The aqueous mixture was frozen to −78 °C and lyophilized to give an off-white powder that was dissolved in water and ion-exchanged for NH_4^+. The ion-exchanged solution was frozen at −78 °C and lyophilized to give 0.026 g of an off-white powder (59.7% pure by CD, impurities were inorganic salts and water): ^{1}H NMR (10% CD_3CN/90% borate-*d*) δ (ppm) 7.32 (s, 12H), 7.19 (d, 6H), 7.03 (d, 6H), 6.55 (dd, 6H), 5.20 (s, 6H), 5.09 (s, 12H).

4-Octaacid. In a 25 mL flask 0.016 g (1.17×10^{-5} mol) of 4-octamethyl ester was dissolved in 12 mL of THF, followed by addition of 0.057 g (3.79×10^{-4} mol) of cesium hydroxide and 3 mL of water. The mixture was allowed to stir in the dark at room temperature overnight, and the THF was removed by rotary evaporation. The aqueous mixture was frozen to −78 °C and lyophilized to give an off-white powder that was dissolved in water and ion-exchanged for NH_4^+. The ion-exchanged solution was frozen at −78 °C and lyophilized to give 0.030 g of an off-white powder (67.2% pure by CD, impurities were inorganic salts and water); ESMS (anion mode, material in cesium borate) *m/e* 212 (M^{8-}).

2, 6-Bis(*p*-methybenzyloxy)-9,10-dihydro-11,12-dicarboxyethenoanthracene (Diacid) (5). In a 50 mL flask 0.018 g (3.38×10^{-5} mol) of 5-dimethyl ester (preparation below) was dissolved in 10 mL of THF, followed by addition of 0.049 g (3.27×10^{-4} mol) of cesium hydroxide and 2.5 mL of water. The mixture was allowed to stir in the dark at room temperature overnight, and the THF was removed by rotary evaporation. The aqueous mixture was frozen to −78 °C and lyophilized to give a white powder that was dissolved in water and ion-exchanged for NH_4^+. The ion-exchanged solution was frozen at −78 °C and lyophilized to give 0.020 g of a white powder (78.3% pure by CD, impurities were inorganic salts and water): ^{1}H NMR (borate-*d*) δ (ppm) 7.34 (d, 4H, $J = 6.0$ Hz), 7.32 (d, 4H, $J = 5.6$ Hz), 7.25 (d, 2H, $J = 7.9$ Hz), 7.11 (d, 2H, $J = 1.8$ Hz), 6.62 (dd, 2H), 5.28 (s, 2H), 4.98 (AB, 4H), 2.33 (s, 6H).

2, 6-Bis(*p*-methybenzyloxy)-9,10-dihydro-11,12-dicarbomethoxyethenoanthracene (5-Dimethyl Ester). A 25 mL oven dried flask was charged with 0.012 g (3.40×10^{-5} mol) of **8**, 0.020 g (1.08×10^{-4} mol) of α-bromo-*p*-xylene, and 0.054 g (1.65×10^{-4} mol) of cesium carbonate. After addition of 10 mL of acetonitrile, the mixture was heated to 55 °C and allowed to stir in the dark. After 18 h TLC (silica gel, 3:1 ether:petroleum ether) indicated completion of the reaction, and the mixture was filtered and purified by flash chromatography (material placed on silica gel plug, 1:1 ether:petroleum ether): obtained 0.0176 g (98%) of product; ^{1}H NMR ($CDCl_3$) δ (ppm) 7.21 (d, 4 H), 7.16 (d, 4 H), 7.05 (d, 2H), 7.02 (d, 2H), 6.54 (dd, 2H), 5.30 (s, 2H), 4.93 (s, 4H), 3.76 (s, 6H), 2.33 (s, 6H); CD [(*R,R*)-enantiomer, CH_3CN] λ ($\Delta\epsilon$) [nm (M^{-1} cm^{-1})], 318 (+2.3), 301 (−0.8), 286 (+17.6), 250 (−53.1), 230 (+102.4), 216 (−2.5), 207 (+52.1).

2,6-Bis(methoxy)-9,10-dihydro-11,12-dicarboxyethenoanthracene (Diacid) (6). In a 10 mL flask 0.015 g (3.94×10^{-5} mol) of 6-dimethyl ester (preparation below) was dissolved in 4 mL of THF, followed by addition of 0.06 g (3.96×10^{-4} mol) of cesium hydroxide and 1.0 mL of water. The mixture was allowed to stir in the dark at room temperature overnight, and the THF was removed by rotary evaporation. The aqueous mixture was frozen to −78 °C and lyophilized to give a white powder that was dissolved in water and ion-exchanged for NH_4^+. The ion-exchanged solution was frozen at −78 °C and lyophilized to give 0.022 g of an off-white powder (69.1% pure by CD, impurities were inorganic salts and water): ^{1}H NMR (Borate-*d*) δ (ppm) 7.36 (d, 2H, $J = 7.6$ Hz), 7.13 (d, 2H, $J = 2.3$ Hz), 6.63 (dd, 2H, $J = 2.4$, 7.4 Hz), 5.31 (s, 2H), 3.77 (s, 6H).

2,6-Bis(methoxy)-9,10-dihydro-11,12-dicarbomethoxyethenoanthracene (6-Dimethyl Ester). A 25 mL oven dried flask was charged with 0.051 g (1.45×10^{-5} mol) of **8** and 0.234 g (7.46×10^{-4} mol) of cesium carbonate. After addition of 10 mL of acetonitrile, methyl iodide (0.1 mL, 0.228 g, 1.60×10^{-3} mol) was added dropwise. The mixture was heated to 50 °C and allowed to stir in the dark. After 6 h TLC (silica gel, 1:1 ether:petroleum ether) indicated completion of the reaction, and the mixture was filtered and purified by flash chromatography (material placed on silica gel plug, 1:1 ether:petroleum ether): obtained 0.06 g (quantitative yield) of product; ^{1}H NMR ($CDCl_3$) δ (ppm) 7.23 (d, 2 H), 6.95 (d, 2H,), 6.47 (dd, 2H), 5.31 (s, 2H), 3.79 (s, 6H), 3.76 (s, 6H); CD [(*R,R*)-enantiomer, CH_3CN] λ ($\Delta\epsilon$) [nm (M^{-1} cm^{-1})], 318 (+2.6), 302 (−1.4), 285 (+16.2), 250 (−46.6), 229 (+71.0), 217 (−1.1), 205 (+72.6).

2,6-Bis[*p*-(dimethylamino)benzoyloxy]-9,10-dihydro-11,12-dicarbomethoxyethenoanthracene (10). A 25 mL oven dried flask was charged with 0.024 g (6.81×10^{-5} mol) of **8**, 0.065 g (3.54×10^{-4} mol) of *p*-(dimethylamino)benzoyl chloride (preparation below), 50 μL (0.05 g, 6.18×10^{-4} mol) of pyridine, and a catalytic amount of DMAP. The mixture was dissolved in 5 mL of THF and heated to 55 °C with stirring in the dark. After 19 h TLC (silica gel, 7:3 CH_2Cl_2:ether) indicated completion of reaction. The mixture was filtered, and the filtrate rotary evaporated to give a yellowish residue; two consecutive purifications by flash chromatography (Si gel, 7:3 CH_2Cl_2:ether) provided 0.035 g (80%) of **8**: ^{1}H NMR (CD_3CN) δ (ppm) 8.12 (d, 4H, $J = 8.6$ Hz), 7.48 (d, 2H, $J = 8.3$ Hz), 7.38 (d, 4H, $J = 8.6$ Hz), 7.33 (d, 2H, $J = 2.2$ Hz), 6.91 (dd, 2H, $J = 8.3$, 2.3 Hz), 5.63 (s, 2H), 3.75 (s, 6H), 3.09 (s, 12H); FAB-MS, *m/e* 647 (MH^+), 312, 180, 166, 148, 122; HRMS, 664.2659 ($M + NH_4^+$), calculated for $C_{38}H_{34}N_2O_8 + NH_4^+$ 664.2660; CD [(*R,R*)-enantiomer, CH_3CN] λ ($\Delta\epsilon$) [nm (M^{-1} cm^{-1})], 324 (+35.0), 295 (−6.2), 270 (+4.9), 247 (−9.4), 218 (+42.3).

***p*-(Dimethylamino)benzoyl Chloride.** A suspension of phosphorous pentachloride (12.61 g, 0.061 mol) in 225 mL of carbon disulfide was added slowly to a stirring suspension of 10.04 g (0.061 mol) of *p*-(dimethylamino)benzoic acid and 5.4 mL (5.28 g, 0.067 mol) of pyridine in 100 mL of carbon disulfide over a 1 h period. Upon complete addition the mixture was heated at reflux until all the white solid dissolved after which the mixture was filtered (CAUTION−CS_2 is very flammable) and allowed to cool. The white crystals that formed on cooling were collected and dried under vacuum in a desiccator to yield 5.52 g (50%): ^{1}H NMR ($CDCl_3$) δ (ppm) 7.95 (d, 2H, $J = 9.12$ Hz), 6.71 (d, 2H, $J = 9.4$ Hz), 3.15 (s, 6H); IR (KBr) 1737 cm^{-1} (COCl); GC/MS 21 min *m/e* 120 (M − COCl).

Guests. Guests **14**, **16**, **17**, **18**, **19**, **24**, **26**, **27**, **28**, **29**, **30**, **31**, **32**, **33**, **34**, **35**, and **36** were obtained from commercial sources. Guests **15**[55] and **25**[56] were prepared as described in the literature. Guests **11**, **12**, **13**, **20**, **21**, **22**, and **23** were prepared through alkylation of the appropriate amine, quinoline, or isoquinoline with methyl iodide. Chloride salts were obtained by ion exchange of the appropriate iodide or bromide salt using Dowex 1 × 8−400 ion exchange resin. Guest purity of hydroscopic guests (all the chloride salts) was ascertained from elemental analysis. Guests were used as is unless elemental analysis, NMR, or UV/vis spectroscopy indicated the presence of organic impurities; in such cases further ion exchange, recrystallization, or other appropriate means of purification was employed, and the samples were checked by elemental analysis.

Computational Studies. Excitonic chirality and induced circular dichroism calculations were set up and executed using Excel.[57] Geometry optimizations with AM1 were done in InsightII.[58] Semi-

empirical calculations of spectroscopic observables were set up and executed using the DZDO program[59] using the Zerner parameter set for the INDO/S model Hamiltonian with the SCF calculations using the closed shell RHF method. CI was limited to singly excited states.

Calculation Controls. The calculations of expected induced CD all involve guest transition moments placed in an ideal orientation, i.e., in the *xz*-plane, centered at the origin, etc. We know from NMR studies that all of our guests undergo rapid exchange between free and bound states, thus the position of the guest transition moment is not as restricted as the calculation assumes. A series of control calculations using a "generic" guest transition moment were carried out in which ν was decreased with μ remaining constant (f decreases), ν was decreased with μ increasing (f remains constant), f increased at a constant ν, the transition moment midpoint offset from the origin along z-axis, and the transition moment was kept parallel to the z-axis but moved off the z-axis by x-axis translation. In each case the transition moment in the xz-plane was rotated about the y-axis as in the previous calculations. The most significant effect on the sign of R was associated with variation of ν. A decrease in ν (increase in λ of transition) results in a shift of R toward more negative values. Other controls involving variations of the angle of inclination from x- and y -axes show that significant sign changes will only occur in guest orientations that are not possible with the rhomboid host cavity. Based on these controls and the agreement of calculation and experiment, we are confident of the validity of our calculations.

Molecular Mechanics Calculations of (*R,R*)-10. The atomic coordinates for (*R,R*)-**10** were obtained from BIOGRAF[26] with the AMBER force field.[27] AMBER is not parametrized for a $N_{(amine)}-C_{(aromatic)}$ bond, so for purposes of calculation the dimethyl amino group was replaced with a 2-propyl group. Six torsion angles involving the benzoates were varied from 0°−180° using a 1000 step Monte-Carlo search with 200 minimizations at each step. A total of 1000 possible structures were searched by a usage directed method,[28] and all structures within 6 Kcal of the lowest energy conformation were saved. In an effort to save computational time, energy was checked after the first 100 minimizations, and if the best structure was 12 Kcal above the previous best structure, it was discarded. This gave 553 low energy structures which were resubmitted for further minimization, and duplicates were identified and eliminated by superimposing of heavy atoms resulting in deviations in overlap of less than 0.25 Å. The result was 64 structures within 1.2 Kcal of one another. The excitonic chirality calculations[25] on these 64 structures all predicted positive excitonic chirality (positive first Cotton effect, negative second Cotton effect). This observation was experimentally confirmed.

CD Data for Previously Reported Compounds. 2, 6-Dihydroxyethenoanthracene (6): [(*R,R*)-enantiomer, CH_3CN] λ ($\Delta\epsilon$) [nm (M^{-1} cm^{-1})], 302 (−3.5), 285 (+16.4), 250 (−41.9), 229 (+61.3), 217 (−9.0), 206 (+59.8).

1-Tetramethyl Ester: [(*S,S,S,S*)-enantiomer, CH_3CN] λ ($\Delta\epsilon$) [nm (M^{-1} cm^{-1})], 297 (+14.0), 283 (−2.8), 251 (+144), 227 (−272), 208 (−85.6).

3-Hexamethyl Ester: [(*R,R,R,R,R,R*)-enantiomer, CH_3CN] λ ($\Delta\epsilon$) [nm (M^{-1} cm^{-1})], 320 (+4.6), 298 (−11.4), 285 (+23.7), 251 (−207), 228 (+360), 207 (+145).

4-Octamethyl Ester: [(*S,S,S,S,S,S,S,S*)-enantiomer, CH_3CN] λ ($\Delta\epsilon$) [nm (M^{-1} cm^{-1})], 319 (−12.0), 300 (+2.3), 285 (−52.7), 251 (+224), 229 (−406), 207 (−167).

Acknowledgment. This work was supported by the Office of Naval Research to whom we are grateful. J.E.F. was supported, in part, as a trainee in the NIH Bioorganic/Bioinorganic Training Program. We wish to thank Patrick Kearney, Sandro Mecozzi, Alison McCurdy, Laura Mizoue, Anthony West, Jr., and Leslie Jimenez for providing samples and Josef Michl for allowing us the use of his DZDO program as well as helpful discussions. J.E.F. would like to thank Robert Kumpf and Anthony West, Jr., for their invaluable help in setting up calculations. We are also grateful to the personnel at the mass spectrometry facilities of University of California Riverside and University of California Berkeley for running ESMS (UCB) and FAB/HRMS (UCR) samples.

Supporting Information Available: Detailed descriptions of the assignment of absolute stereochemistry of **8** and **10**, CD spectra of host $\mathbf{2_R}$ with rhomboid and toroid binding guests, full listing of all calculated transitions, oscillator strengths, and transition dipole moment vectors, R vs θ curves for various host−guest complexes described (but not shown) in text, and CD spectra of the $\mathbf{35/3_S}$ host−guest complex (18 pages). This material is contained in many libraries on microfiche, immediately follows this article in the microfilm version of the journal, can be ordered from the ACS, and can be downloaded from the Internet; see current masthead page for ordering information and Internet access instructions.

JA951610F